INSTITUTE OF PHYSICS PUBLISHING PHYSICS IN MEDICINE AND BIOLOGY

Phys. Med. Biol. **51** (2006) R505–R540 doi:10.1088/0031-9155/51/14/R01

TOPICAL REVIEW

Image-guidance for surgical procedures

Terry M Peters

Robarts Research Institute, University of Western Ontario, PO Box 5015, 100 Perth Drive, London, ON N6A 5K8, Canada

E-mail: tpeters@imaging.robarts.ca

Received 12 October 2005, in final form 13 March 2006
Published 23 June 2006
Online at stacks.iop.org/PMB/51/R505

Abstract

Contemporary imaging modalities can now provide the surgeon with high quality three- and four-dimensional images depicting not only normal anatomy and pathology, but also vascularity and function. A key component of image-guided surgery (IGS) is the ability to register multi-modal pre-operative images to each other and to the patient. The other important component of IGS is the ability to track instruments in real time during the procedure and to display them as part of a realistic model of the operative volume. Stereoscopic, virtual- and augmented-reality techniques have been implemented to enhance the visualization and guidance process. For the most part, IGS relies on the assumption that the pre-operatively acquired images used to guide the surgery accurately represent the morphology of the tissue during the procedure. This assumption may not necessarily be valid, and so intra-operative real-time imaging using interventional MRI, ultrasound, video and electrophysiological recordings are often employed to ameliorate this situation. Although IGS is now in extensive routine clinical use in neurosurgery and is gaining ground in other surgical disciplines, there remain many drawbacks that must be overcome before it can be employed in more general minimally-invasive procedures. This review overviews the roots of IGS in neurosurgery, provides examples of its use outside the brain, discusses the infrastructure required for successful implementation of IGS approaches and outlines the challenges that must be overcome for IGS to advance further.

(Some figures in this article are in colour only in the electronic version)

1. Introduction

Image-guidance is used in surgery in much the same manner that modern navigational technology is employed to guide an airline pilot at night through unfamiliar terrain or bad weather. In either case, a direct view of the landing site (target) may be unavailable, and so

navigation is achieved with respect to a model of the environment, rather than via a direct view. The model is often complemented by real-time information such as weather conditions, altitude and glide-path. Image-guided surgery employs a similar paradigm, using information acquired from a variety of imaging sources. As reported by Webb (1988), one of the first recorded uses of a medical image being employed 'with clinical intent' was in Birmingham (UK) on the 13th January 1896 to visualize a needle in a woman's hand. A month later, John Cox, Professor of Physics at McGill University in Montreal (Cox 1896) successfully removed a bullet from the leg of a victim based upon the radiograph that had been made of the limb. Not only was the projectile successfully removed on the basis of the radiograph, it was later used as evidence during a suit against the man who had shot the victim! Bearing in mind that Roentgen 'discovered' x-rays on 8 November 1895 (Dam 1896), these uses of radiography in medicine must surely represent the most rapid translation ever of a scientific discovery into clinical practice.

Many surgical interventions involve significant trauma to the patient just to access the target of the surgical or therapeutic procedure. In fact, in many instances, the 'surgery' is barely related to the target at all. Consider conventional coronary artery bypass surgery (CABG). In order to reach the target (vessels for anastomosis), the patient's rib-cage is opened, the heart isolated from the body's circulatory system, and the patient kept alive by a heart–lung machine. In CABG, the actual anastomosis is a relatively benign procedure, compared to the trauma-inducing process of accessing the target. While this example is extreme, it nevertheless illustrates why minimally-invasive procedures, complemented with image-guidance, are becoming increasingly desirable. Another example is the therapy for Parkinson's disease and other movement disorders. The necessary target is a small number of cells within the brain occupying a volume of fractions of a cubic millimetre. To ensure minimal trauma to the patient, these regions must be targeted accurately and approached by a route that offers minimal disturbance to intervening tissue.

This paper provides an overview of the roots of image-guidance in neurosurgery, and discusses its use both within the brain and in other areas of the body. It also outlines the infrastructure required for successful implementation of IGS approaches along with the challenges that must be overcome for IGS to advance further.

2. Stereotactic surgery

2.1. Frames

The stereotactic frame forms the reference gold-standard for image-guided neurosurgery. Although there are many different frame designs available, they all perform the same basic functions of providing a robust rigid reference system that establishes a coordinate system relative to the patient, delivering recognizable landmarks in the images, and serving as a stable mounting base and instrument guide (figure 1). The differences in the frame lie in the manner in which the trajectory to the target point is specified, and the way in which they are fastened to the head. Some frames employ a simple orthogonal system where trajectories are constrained to be parallel to the sides of the square base of the frame, while others use a more sophisticated arc-based system. In the latter type of frames, the target is always positioned at the isocentre of an arc used to hold the instruments. Such an arc allows the target to be approached with any azimuthal or declination angle, with the assurance that the trajectory will always intersect the target. In the absence of real-time tracking of surgical probes, the scales marked on the frame also allow the position of the instrument to be established by reference to a frame-based coordinate system.

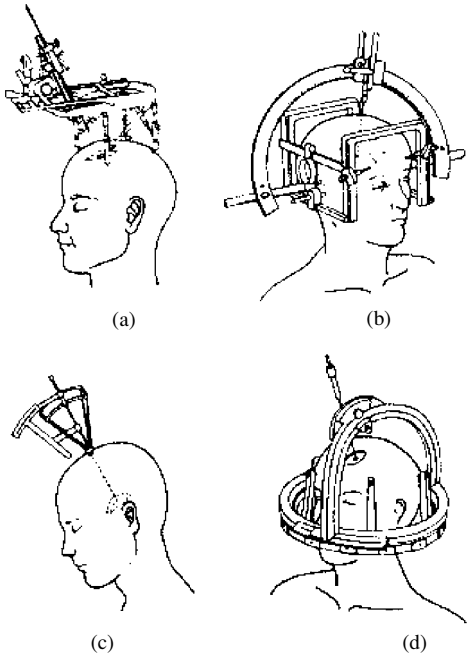

Figure 1. Schematic representations of several classes of stereotactic frame. (a) Translational system, (b) arc centred system; (c) burr-hole mounted system and (d) interlocking arc system. (From figures 1–4 by Gildenberg P L 1998 The history of stereotactic and functional neurosurgery *Textbook of Functional and Stereotactic Neurosurgery* ed P L Gildenberg and R Tasker (New York: McGraw-Hill) Used with permission.)

What we understand today as image-guided surgery (IGS) has its roots in stereotactic neurosurgical surgical procedures developed early in the 20th century by Horsley and Clarke (1908). These techniques provided the necessary spatial referencing system that permitted unique markings fixed to the patient to be visualized on an image, enabling a transformation between 'patient-space' and 'image-space' to be established. Horsley and Clarke used Cartesian coordinates to establish the positions of target points within a monkey brain, relative to fixed landmarks on the skull itself. According to Levy (1992), while the idea behind this technique led to a patent for a human apparatus, several years elapsed before it saw clinical use, when Aubrey Mussen, an engineer who had worked with the Horsley–Clarke system, designed a similar device for the human skull (Olivier *et al* 1983). This apparatus was discovered some 30 years after Mussen's death, wrapped in a newspaper dated 1918 which is presumably the year it had been constructed. Spiegel *et al* (1947) further developed the technique of stereotaxy, using the concept of a three-dimensional Cartesian coordinate system for the human brain. These coordinates were defined with respect both to the brain, and to radiographic images acquired while the patient was fitted with a reference (or stereotactic) frame attached to his head.

Many teams developed various frame designs, and during the 1950s over 40 other examples of stereotactic systems appeared (Guildenberg 1988). All of these combined the referencing system of the frame with mechanical devices to guide a probe to deep brain structures, and allowed the position of the target to be described in terms of a frame-based coordinate system. Image-guided surgery, particularly in the brain, may still be frame based,

but modern tracking technology has enabled IGS to be used in further applications without the read of a stereotactic frame. The development and evolution of stereotactic surgery, and its impact on the more general field of image-guided surgery outside the brain, is discussed at length by Galloway (2001).

2.2. Imaging

While x-ray imaging may allow a bullet or needle to be visualized easily, showing differentiation between bone and soft-tissue, it cannot distinguish targets within the soft tissue of the human brain. The major difficulty is that a radiograph of the human head shows only a projection of the bony skull, and the small contrast differential in transmitted x-ray intensity provided by brain tissue does not register on film. Unless an intracranial abnormality results in deformed bone-structure, standard radiographs are of no practical use for detecting the presence of anomalies. To provide improved intracranial visualization, two techniques, pneumo-encephalography and ventriculography were developed, both involving the introduction of a contrast medium into the cerebral ventricles. In pneumo-encephalography, the contrast medium was air, while ventriculography used an x-ray opaque radiographic contrast. Even then, the visualization of tumours could only be achieved by indirect inference of changes in the normal appearance of the ventricles by space-occupying lesions, and conventional radiography still played an important role. Nevertheless, ventriculography was still occasionally used for accurately outlining the ventricles, usually in conjunction with other imaging modalities during image-guided surgery (Alterman *et al* 1995, St-Jean *et al* 1998).

Standard radiography has two limitations. Firstly, it provides projections through the body and the three-dimensional information contained within is reduced to two, resulting in the loss of information about the dimension parallel to the beam. Secondly, x-rays diverge from a point source, so there is a differential magnification factor that distorts the perceived sizes of imaged structures. This makes it difficult to directly measure structure size, or to determine distances to, or between target points by direct examination of the x-ray image. This latter objection can be overcome to some extent by constructing a very long focal-length ($\sim$9 m) x-ray system, such that the rays are effectively parallel as they pass through the patient. Under these conditions of minimal differential magnification, coordinates of the target within the brain may be measured from the radiographs directly with minimal error. This arrangement was employed by a number of centres to make intra-operative orthogonal anterior–posterior (AP) and lateral radiographs, and allowed the 3D coordinates of structures located uniquely in the two images to be measured with a ruler.

The advent of tomographic imaging with CT in the 1970s sparked a renewed interest in the development of image-guided stereotaxy. Bergstrom and Greitz (1976) described their early experience of CT using stereotactic frames, and this was followed by many other reports describing the adaptation of CT to stereotactic surgery. Brown (1979) formally outlined a configuration of fiducial markers attached to the frame that could be imaged with CT, and which could be recognized in the images. Brown described the methodology of establishing the frame coordinates of any pixel in the image, based on the locations of the markers in the images. The configuration of parallel and oblique rods surrounding the frame form the basis of frame-mounted stereotactic fiducial markers currently in use.

Today, stereotactic frames may be equipped with two types of fiducial markers. The first is designed to be imaged by a tomographic system and generally consists of a series of ‘Z’, ‘N’ or ‘V’ bars mounted on the frame. Their configuration is such that when they are intersected by the image slices, their imaged configuration is unique for any slice (figure 2).

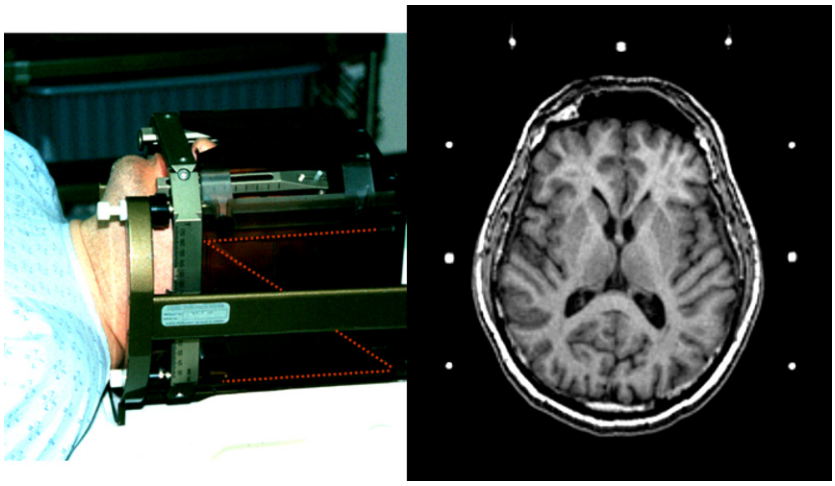

(a) (b)

Figure 2. (a) Stereotactic frame attached to a patient with fiducial marker bars shown by the dotted lines. (b) White dots are the representations of these markers in the images.

If a slice contains at least three sets of markers, its oblique position within the volume may be determined unambiguously. While registration of an entire three-dimensional volume can be achieved with a minimum of just three points within the volume, the stereotactic frame predated true 3D imaging modalities, and planning was generally performed manually on a slice-by-slice basis.

An alternative fiducial marker configuration, comprising two sets of point objects on frame-mounted plates perpendicular to the central rays of lateral and anterior–posterior x-ray beams, was designed to be used with x-ray projection images. Each of these points appears clearly in the projection images, and their positions can be used to precisely determine the imaging geometry. Using this approach, three-dimensional localization of structures within the body may be achieved using orthogonal (or even stereoscopic) image pairs (Henri *et al* 1991b)

3. Computers in image-guided surgery

For many years, image-guided surgery was confined to stereotactic procedures and was performed without the use of a computer (apart from that employed by the scanner to reconstruct the image). Transparent templates were simply placed on the display monitor, with patterns aligned with the fiducial markings on the image, and the coordinates read off directly. Many years prior to the advent of CT, specialized laboratories were using computers in conjunction with x-ray ventriculography and brain atlases to plan stereotactic neurosurgery procedures. The work by Bertrand *et al* (1974) and Thompson and Bertrand (1972) set the stage for many of the computer-assisted surgery applications that have subsequently evolved.

In the early 1980s, computerized planning systems were introduced to establish frame-related coordinate systems based on fiducial markers that were recognized on a slice-by-slice basis in CT and MR images. Initially, these programs ran on the CT or MRI computers (Peters *et al* 1986), which typically were 16-bit ‘minicomputers’. In the late 1970s, systems with 128K of memory and 5 MB of disk storage were typical. As computer hardware become

cheaper and more widely available, independent systems evolved that could read images from different modalities, and from scanners supplied by different manufacturers (Hardy and Koch 1982, Hardy *et al* 1983, Peters *et al* 1986). Since the mid 1980s, the evolution of the DICOM standard (Clunie 2006) has largely, (although not entirely) eliminated the problems of data incompatibility between manufacturers.

Since each imaging modality provides its own unique information, it was logical to combine the images from multiple imaging devices so that surgical planning could make use of the information from MRI, CT, angiography and PET/SPECT images. Such multi-modality imaging was considered important for certain procedures, such as the insertion of probes or electrodes into the brain. For example, using MRI and DSA images, the pathway to a target could be planned with the knowledge that it traversed a vascular-free zone, either by using orthogonal projections or stereoscopic image pairs depicting the vascular system (Peters *et al* 1994). While the majority of stereotactic procedures were concerned with the introduction of probes, cannulae or electrodes into the brain, Kelly (1986, 1991), and Morita and Kelly (1993) proposed an innovative application for the treatment of intracranial intra-axial neoplasms. Instead of a narrow cannula, Kelly employed a cylindrical retractor integrated with a stereotactic frame to approach a volumetric lesion. Such stereotactally localized tumours could be biopsied and treated by the stereotactic implantation of radionuclide sources or resected using computer-assisted stereotactic laser microsurgical techniques. Kelly's work provided the linkage between conventional frame-based stereotactic neurosurgery, and the frameless approaches that subsequently evolved.

4. Image registration

For many years, stereotactic frames provided the means of registering the patient to the images. The use of a frame generally involves a minimally invasive surgical procedure to fasten it to the patient (either by creating 3–4 1–2 mm deep holes in the skull with a twist-drill to accept blunt pins, or by using sharp pins applied to the skull under pressure). The frame (or at least a removable base-ring) can often be intrusive in the operating room, so there was a general desire to dispense with the frame entirely. However, without a frame to provide the fiducial markers, some other sort of reference system was necessary to register the patient to the image(s).

4.1. Point matching

Frameless registration of pre-operative images to the patient can occur in a variety of ways. The most common require that homologous structures be identified in both the images and on the patient. One approach employs a computer-tracked pointer to identify patient landmarks such as the outer canthi of the eyes, the tragus of the ears and the nasion. These same structures are then identified via a cursor within the three-dimensional image(s) of the patient. While widely used, this approach has its limitations. Firstly, since it is difficult to precisely identify the locations of the landmark points on the patient, there is bound to be some error with respect to their homologues on the images. Because of this, the best one can hope to achieve is a least-squares approximation to the correct registration. Of course, as long as there is no systematic bias error in identifying the landmarks on the patient or in the images, the accuracy of such a registration will asymptotically improve as the number of homologous points is increased. In addition, if all the registration points are clustered towards one side of the head, a small registration inaccuracy in the region containing the homologous points can result in a magnified error at remote points, a phenomenon that has been discussed at length by Maurer and colleagues (Fitzpatrick *et al* 1998, Maurer *et al* 1997a, 1998).

4.2. Surface matching

Point-based registration is complemented in some systems with surface-matching. Although these procedures are now commonplace, this approach was first described by Pelizzari and Chen (1989) who used surfaces extracted from 3D multi-modality patient images to register these images within a common coordinate system. While they used two digital image volumes, the same procedure can be followed to match the surface extracted from a single volumetric image with physical samples of the same surface of the object. This technique involves using the probe to sample points on the surface of the patient, and then determining the best match of this point-cloud to an extracted surface from the 3D patient image. Maurer *et al* (1998) described this combined approach which is incorporated in some commonly used commercial image-guided neurosurgical systems. Under ideal conditions (i.e. in phantom tests where homologous structures are easily identified and there is no movement of the markers with respect to the object), the accuracy of this technique can approach that of a stereotactic frame (Zinreich *et al* 1993). However, under clinical conditions, where natural features on the patient's skin are identified, the accuracy decreases due to the subjective identification of homologous point-pairs on the patient and in the images. While it may be adequate for many neurosurgical purposes, this registration technique used alone is not appropriate for procedures requiring great precision. This problem becomes more acute when organs outside the brain are to be registered to their images.

4.3. Bone-mounted markers

The accuracy and precision of point matching procedures can be improved by fastening surface markers to the patient's skin. Under such conditions, the markers can be more precisely determined using a tracked pointer, and with appropriate software they can be automatically identified within the patient's three-dimensional images. Even though these markers are fixed to the skin, they can move with respect to the underlying rigid bony anatomy, and therefore add error. Maurer *et al* (1997b) demonstrated convincingly that the only way to achieve patient-to-image registration with an accuracy matching that of a stereotactic frame is to use bone-mounted fiducial markers for image-patient registration. It is often argued that the process of implanting such markers is an invasive procedure akin to the pin-mounting involved in fitting a stereotactic frame, but it can be performed under local anaesthesia and is certainly less invasive than any subsequent surgical procedure. They demonstrated that the registration accuracy and precision obtainable with properly designed markers is in the order of 0.5 to 1.5 mm.

4.4. Image to image registration

4.4.1. 3D to 3D. Originally, the primary imaging modality employed for planning and guiding stereotactic surgical procedures was CT. With the advent of other imaging modalities such as MR, SPECT, PET and DSA that could be registered with the CT volume, it became clear that these additional imaging modalities could complement the information from CT. These additional data could add enhanced soft-tissue information (MRI), locate functionally active regions (PET, SPECT, fMRI) and add vascular data to the anatomical (MR angiography, DSA). For this reason, multi-modality image display and analysis systems were developed to allow the planning and guidance operation to take place using multiple image data sets simultaneously (Henri *et al* 1991a, Hill *et al* 1991, 1994). The key to the deployment of such multi-modality imaging was image registration—a topic that has become a dominant area of research in medical imaging. In many applications, for example mapping atlases to images,

or the registration of pre-operative to intra-operative images, nonlinear image registration is required. The reader is referred to comprehensive reviews on this topic by Maintz and Viergever (1998), Hill *et al* (2001) and Crum *et al* (2003, 2004).

Even though MRI and CT are 3D, and digital subtraction angiography is 2D, a point identified in the 3D modality may be projected into the 2D angiogram. Likewise, a point within a planar angiogram may be represented as a line within the MRI or CT volume. By employing orthogonal or stereoscopic angiogram pairs, three-dimensional localization may be achieved within the angiogram-defined space to assist in the planning of vascular-free trajectories to deep brain structures, or when localizing the foci of epileptic seizures through the implantation of EEG recording electrodes (Olivier *et al* 1994, 1996).

4.4.2. 2D to 3D. Procedures to perform 2D to 3D image registration are becoming increasingly important in real-time guidance situations, and research into accelerating the convergence and improving the accuracy of such methods (Lemieux *et al* 1994, Tomazevic *et al* 2003) has increased dramatically. Much of this work is motivated by the fact that while 3D MR and CT images are of high quality, they cannot be acquired in real time. On the other hand, the real-time imaging modalities (ultrasound and x-ray fluoroscopy) that are available tend to be two dimensional. There is therefore a need to map the real-time 2D image to its 3D pre-operative counterpart in order to combine the quality available from the pre-operative images with the real-time characteristics of the intra-operative data. This procedure involves either finding the pose of the 2D image within the 3D volume (US) or determining the pose of the 3D pre-operative volume whose digitally-reconstructed radiograph (DRR) corresponds to the measured 2D radiograph. A similar situation is faced in mapping dynamic single-slice intra-procedural MR images to pre-operative MR volumes during MR-guided cardiac interventions (Smolikova-Wachowiak *et al* 2005).

Much of the effort in 2D–3D registration research has been put into the rapid computation of the DRR images (Birkfellner *et al* 2005, Russakoff *et al* 2005), reducing the complexity of the search procedure by reducing its dimensionality (Birkfellner *et al* 2003b), and accelerating the optimization procedure (Livyatan *et al* 2003). A similar approach has been employed to address the problem of registering the pre-operative image of a patient's heart to the patient in the OR, through the registration of intra-operative angiograms to vessels in the pre-operative data (Turgeon *et al* 2005). While these image registration techniques are computationally intensive, as demonstrated by Wachowiak and Peters (2006), optimization approaches used for image registration can benefit from parallelization.

5. Coordinate transformations

Image-guided surgery systems must relate the measurements made in one coordinate system (or frame of reference) to those of another. When dealing with the head (and image) in a stereotactic frame, this is relatively straightforward, since the coordinate system of the images is generally aligned with that of the frame. However, when the orientation of the coordinate system etched onto the frame bears no relationship to the reference frame in which the image was acquired, the transformation that maps one coordinate system into the other must be computed. In a typical application, the tracking of a probe or an ultrasound transducer for example, several coordinate transformations may be needed before the images recorded by the transducer can be properly registered with the image of the patient. Figure 3 illustrates the concatenation of the individual transformations, which when combined constitute the global transform. Occasionally it is necessary to display the image of the tracking device within both

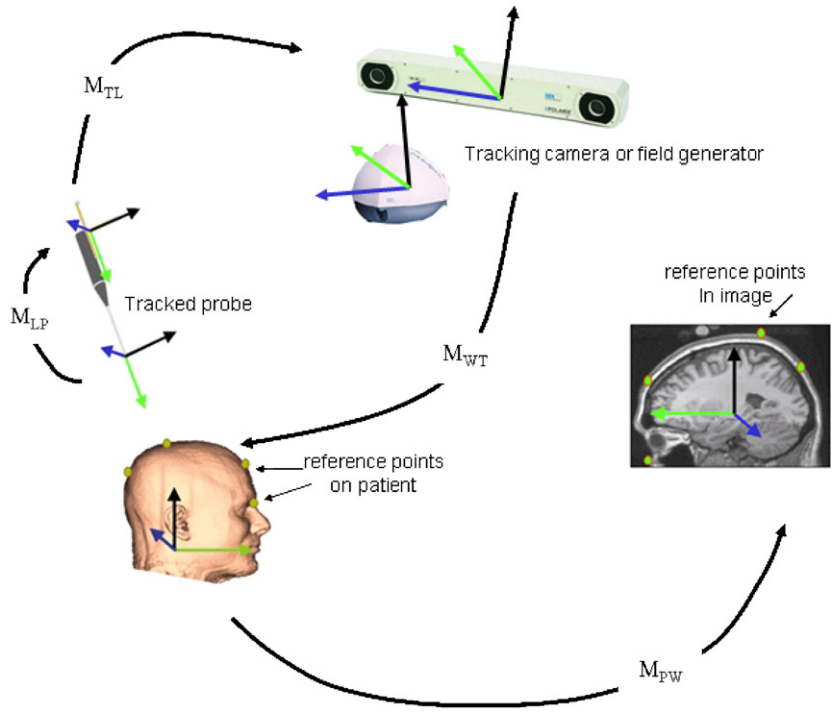

Figure 3. Spatial transforms: several transformation matrices must be computed to enable the tracking of an intra-operative tool, and relate its position to the patient's image: M_{TL} represents the transform between the coordinate system of the optical tracking device, and the LED infra-red emitters or passive reflective balls on the tracked probe. M_{LP} relates these emitters to the probe tip (or other instrument being tracked); M_{WT} is the transform between the tracking device and 'world' coordinates (the patient), and M_{PW} is the transform that maps the patient coordinate system to the image. Each of these transformation matrices must be carefully determined from calibration procedures.

a 2D projection image (DSA for example) and a 3D image (MRI). In the DSA case the image is a diverging-ray projection through the 3D object. In this case, a homogeneous transformation matrix (Henri *et al* 1991a) performs a 'many-to-one' transform when mapping between the 3D and 2D images (i.e. multiple points in the 3D image map into a single point in the 2D image). Conversely, a one-to-many transformation is computed when mapping a point in the 2D image into a line in 3D.

6. Tracking systems

To a large extent, stereotactic procedures as described above are used during the planning stage of a surgical procedure. In some surgical procedures, once the target and trajectory are determined, there is no further need for image-guidance during the procedure. However, if guidance (i.e. knowing precisely where the instrument is located with respect to the target at all times during the procedure) is required, then probes and instruments must be tracked and related to the patient images. The tracking system is therefore an essential component of any intra-operative image-guidance system.

Some mechanical tracking approaches employ a probe that is physically linked by a multi-jointed arm to the apparatus restraining the patient's head, and the position of the probe is determined by sensing the angles at each joint (Golfinos and Spetzler 1996, Zinreich *et al* 1993). Alternatively, there are ultrasonic, optical (Reinhardt *et al* 1998), or magnetic (Birkfellner *et al* 1998a, 1998b, Frantz *et al* 2003) methods to determine the probe's position. Each system has its advantages and drawbacks. While mechanical systems are always in communication with the computer and do not rely on uninterrupted sight-lines between the probe and the signal transducer, they tend to be bulky and more intrusive in the operating room. For these reasons, the use of mechanical tracking systems has diminished in routine clinical use for IGS.

The limitations of mechanical systems are overcome by magnetic, ultrasonic and optical techniques, but the latter two approaches must have unobstructed sight-lines between sensors on the probe and some transmitting device. Magnetic systems do not suffer from this limitation, but their performance is often limited by the presence of metal in the vicinity of the pulsed magnetic field transmitter, or the magnetic field sensors. Some efforts have been made to combine optical and magnetic devices, with a design that uses an optically tracked system to re-calibrate a magnetically based tracker in real time. When sight-lines are broken, the magnetic tracker takes over from the optical system (Birkfellner *et al* 1998b, Hummel *et al* 2005).

The tracking technique most frequently employed in image-guided surgery procedures uses the optical approach, and these devices generally achieve a tracking accuracy and precision of better than 0.5 mm (Wiles *et al* 2004). Some of the more recent optical systems use passive tracking technology where retro-reflecting spheres or even geometric patterns attached to the probe are recognized by a multi-camera optical imaging system (Claron Technologies 2005).

These methods work well for most surgical instruments, but there are no entirely satisfactory solutions to the problem of tracking the position and direction of a catheter tip or a flexible endoscope within the body unless one employs a real-time imaging system such as MRI (Erhart *et al* 1998, Shimizu *et al* 1998, Steiner *et al* 1997), ultrasound (Comeau *et al* 1998, Fenster *et al* 2004, Kaspersen *et al* 2003b) or fluoroscopy (Baert *et al* 2004). Recent work (Frantz *et al* 2003, Hummel *et al* 2002, Wood *et al* 2005) on miniature magnetic sensors (approximately 1 mm diameter by 3 mm in length) is showing promise for tracking flexible devices within the body. Another technology that ultimately may be useful in tracking situations in general, and in flexible endoscopes and catheters in particular, employs fibre-optics. Specially treated optical fibres can be manufactured such that the optical transmission is a function of the radius of curvature of the fibre. This concept has been incorporated into a commercial shape-measuring device 'Shape-tape®'(Danisch *et al* 1999) that allows the shape of a stiff ribbon to be constantly monitored in three-dimensional space. However, this potentially useful technique is hampered by hysteresis, repeatability and lag effects that reduce its suitability for IGS.

7. Tissue motion correction

7.1. Tissue movement during image-guided procedures

Although most stereotactic neurosurgical procedures assume the effect of brain shift to be minimal, this is not true of procedures that require a craniotomy, since the morphology of the brain can change dramatically after the opening of the skull, due to pressure, gravity and fluid drainage effects. In these cases, the surgeon must contend with additional sources of error that are not accounted for during the image-to-patient registration step.

7.2. Brain-shift measurement

It is perhaps surprising, given the potential impact of brain shift during image-guided neurosurgery, that so little attention had been paid to the problem of quantifying its effect until recently. A number of investigators (Hill *et al* 1998, Roberts *et al* 1998, Roberts and Darcey 1996) have addressed this problem and demonstrated that tissue shifts of up to 20 mm can be observed under routine surgical conditions depending on the procedure.

(Maurer *et al* 1998) assessed the extent of tissue motion by comparing pre-operative MR images with intra-operative MR images. They measured brain shifts of up to 5 mm, and ventricular volume changes of up to 44%. Hill *et al* (1998) used a tracked surgical microscope to observe the displacement of reference points on the cortex after craniotomy, and reported median tissue displacements on five patients of up to 7.4 mm. In a study of 28 patients using a tracked surgical microscope to measure the shift of identifiable points on the cortex, Roberts *et al* (1998) observed mean displacements of 10 mm, and shifts of up to 24 mm from their positions as defined by pre-operative MR scans.

7.3. Correction for intra-surgical brain shift

Concurrent with the efforts to measure tissue shift, a number of authors have developed procedures to correct the distortion that takes place during open-craniotomy surgical procedures. Two of these attempt to predict changes in brain shape on the basis of the anticipated effect of drugs, and the observed changes to the cortical surface. The first of these methods by Miga *et al* (2000) predicts the effect of drugs and pressure changes on the drainage of fluid from the brain, and the effect of tissue movement under the influence of gravity. They developed finite element models of brain tissue incorporating both mechanical properties and the manner with which it retains fluid. A second approach scans the surface of the cortex with a laser range-finder and matches the measured surface map with the cortical surface as determined from a pre-operative MR image (Audette *et al* 2000). As the shape of the cortex is observed to change during surgery, the MRI-derived cortical model is deformed to match the surface as measured by the laser scanner. This deformed surface is propagated through a volumetric, finite element representation of the brain structure to predict the extent of the tissue distortion throughout the volume. Miga *et al* (2003) recently extended this technique using a surface scanner that combines distance and texture maps to optimize the registration of the scanned surface representation and the MRI-derived cortex.

A third method (discussed later in the 'interventional imaging' section) uses ultrasound images acquired during surgery to correct the pre-operative MR or CT images.

7.4. Correction of motion in 'unconstrained' organs

Because of the relatively small amount of brain shift encountered during neurosurgery, the brain is an obvious candidate for image-guidance, and as discussed above, the problems of tracking deformations of the brain during surgery can be addressed in a relatively straightforward manner. For similar reasons, orthopaedic surgery has embraced image-guided techniques (DiGioia *et al* 1998, Moulder *et al* 2003, Sugano 2003, Tonet *et al* 2000). When one ventures to other parts of the body, the tracking of, and correction for organ movement is of paramount concern, and lack of robust solutions has limited the use of image-guided approaches in these areas. If minimally-invasive procedures are to be extended successfully to multiple body regions, this problem must be addressed. Most existing work in this area reported to date has been in predicting the movement of abdominal organs due to breathing.

A number of recent publications have addressed the problem of image-guided surgery in the liver (Appelbaum *et al* 2005, Cash *et al* 2003, Herline *et al* 1999, Mevis 2005, Tokuda *et al* 2004, Vetter *et al* 2002), and recent research has tried to characterize the motion of the liver during respiration (Clifford *et al* 2002). Image-to-patient registration is key to performing any procedure that relies on pre-operative images for intra-procedural guidance. In the liver, it is difficult to identify specific landmarks upon which to base such a registration. Herline *et al* (2000) addressed this problem (in an open procedure) by digitizing the surface with an optically-tracked pointer and fitting the obtained cloud of points to the segmented liver surface from a CT scan. They reported a target registration error for simulated tumours of ∼3 mm based on this technique. Cash *et al* (2003) extended this approach by employing a laser-based surface scanner to achieve a similar objective, while at the same time reducing the target registration error to better than 2 mm. This approach offers the added advantage that morphological changes occurring to the liver during the procedure can be tracked and potentially used to drive a deformable-model-based correction strategy.

A small number of centres have MR imagers located in the operating room. These are typically lower field (0.2–0.5 T) open magnets, allowing the surgeon ready access to the patient. While these systems can image the organ intra-operatively (in close to real time) the limitations placed on a open magnet in the OR result in low resolution, poor image quality and high noise. In spite of this, open MRI has proved useful in liver therapy, as demonstrated by Klotz *et al* who performed both cryosurgery (Klotz *et al* 1997b) and interstitial laser therapy (Klotz *et al* 1997a) of the liver under MR guidance in a 0.5 T magnet.

In common with other approaches that employ intra-operative imaging, some groups have found that the image quality and resolution of the open MR systems (particularly at field strengths of less than 0.5 T) are insufficient for direct intra-operative guidance. They have employed non-rigid image registration to map pre-operative acquired high resolution images to those acquired intra-operatively. Carrillo *et al* (2000) evaluated a number of manual and automatic approaches to register pre-operative and intra-operative MR images of the liver, and concluded that a registration accuracy of ∼3 mm could be achieved using a mutual-information based technique.

A more challenging task is to register pre-operative cardiac images to the beating heart for guidance of epi- or endocardiac procedures. Rickers *et al* (2003, 2004) recently reported experience in the use of fused MRI and radiography to perform septal defect repair and stem cell therapy delivery via direct MR fluoroscopy (using a catheter approach in both cases), while Guiraudon (2005) has described a new technique for introducing instruments directly into the cardiac chamber via the heart wall, to perform such procedures as atrial fibrillation ablation, and heart valve and septal defect repair. Practical implementation of this approach will require image fusion and registration similar to that described by Rickers.

8. Atlases

Some minimally invasive surgical procedures require lesions to be made at target points that are related to electrophysiological activity rather than distinct anatomical targets that can be seen directly on the MRI or CT image. The only means of ensuring the lesion is made in the correct position is to perform electro-physiological measurements prior to creating the lesion. The placement of the stimulating or recording electrodes has traditionally relied on standard atlases of the thalamus and globus pallidus. These atlases (Schaltenbrand and Wahren 1977a, 1977b, Nowinski *et al* 1997, 1998, Talairach and Tourneau 1988, 1993) are used as a guide for placing recording or stimulating electrodes within the brain. As the atlases are constructed on the basis of sections made from an individual cadaver brain, they obviously cannot exactly

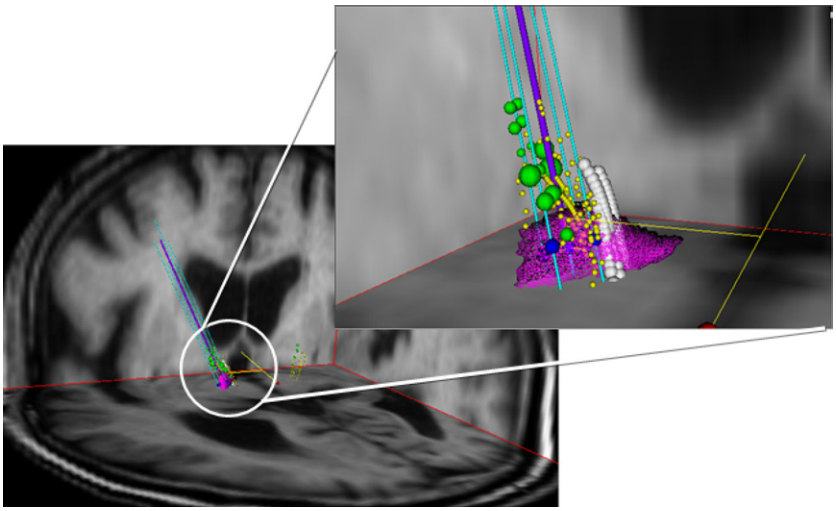

Figure 4. Electrophysiological database imported into surgical planning workstation, showing the region of the brain being targeted within a 3D display, and (inset) the electrophysiological data (small spheres) extracted from a database and mapped to the current patient. Also shown here are the sub-thalamic nucleus and the probes of a five-element recording electrode.

match the brains of individual patients. The practice in the past has been to manually scale individual cross-sectional images from the atlas to match gross features seen in the diagnostic images. Some systems, for example Brain-Bench (Nowinski *et al* 1997, 1998) allow standard atlas images to be integrated directly with the 3D MRI or CT data sets.

St-Jean *et al* (1998) reported the use of a three-dimensional atlas that could be automatically warped to fit the 3D MRI of an individual patient. They created a three-dimensional version of the Schaltenbrand and Wahren atlas which was accurately registered to a 'standard' 3D MRI brain data set. This was subsequently matched, using a nonlinear spatial warping algorithm (Collins *et al* 1995) to the patient's MR images. Using the nonlinear spatial transform calculated by this operation, the three-dimensional atlas was subsequently mapped to the patient. Using this system, target structures within the atlas that define the lesion site may be visualized in three dimensions with anatomical landmarks defined by the 3D MRI, a model of the proposed lesion, and the probe used to create it. While such atlases offer a great deal of assistance to the surgeon, it is still necessary to verify that the lesion is being created in exactly the right place through electrophysiological stimulation and recording. Mis-placing the lesion by as little as 1 or 2 mm could have a disastrous effect on the patient's outcome. The purpose of the atlas, therefore, is not so much to pinpoint the exact target, but to make it easier for the surgeon to approach the desired region quickly and to verify the target position with a minimum of electrophysiological testing. These ideas have been extended by Finnis *et al* (2003) and D'Haese *et al* (2004) with the incorporation of electrophysiological databases (acquired from actual patient populations and registered to the brain volume of the patient under consideration) into the surgical guidance platform as illustrated in figure 4. These electrophysiological data complement the anatomical atlas to improve the precision of the initial target localization.

The ideas embodied in the construction of neurological atlases are slowly being adopted in atlases for other parts of the body. Ehrhardt *et al* (2004) and Tang and Ellis (2005) have employed atlases derived from models of the hip and femur to map to patient anatomy as an aid in surgical planning. Park *et al* (2003) and Qatarneh *et al* (2003) have used atlas techniques

to aid in the segmentation and radiation planning of organs in the abdomen, whilst Frangi *et al* (2002) and Lorenzo-Valdes *et al* (2004) have employed statistical shape models to represent the various components of the heart.

9. Intra-operative imaging

9.1. X-ray fluoroscopy and DSA

While fluoroscopy has been performed for decades to guide catheters during interventions in the brain, it was the introduction of digital subtraction angiography (DSA) in the 1980s (Strother 2000), that provided the foundation upon which the discipline of interventional neuroradiology was based. Using DSA, the vascular system could be seen clearly without the interference of overlying structures, and it provided roadmaps for the treatment of arteriovenous malformations, aneurysms and even stroke. Unfortunately, constant cardiac motion in the heart makes subtraction angiography difficult, but (unsubtracted) x-ray angiography maintains a leading role in the diagnosis and treatment planning of cardiac disease. In situations that do not require real-time imaging, coronary angiography is rapidly being superseded by CT angiography (Schoenhagen *et al* 2005). Fluoroscopy and angiography provide projection images and sometimes are unable to visualize the soft-tissue targets, such as those in the heart. This led to the research described earlier, which combines x-ray fluoroscopy with pre-operative 3D models. By registering the fluoroscopic image with the appropriate view of the 3D model, significant structures (e.g. the tip of a catheter) visualized in the x-ray image may be back-projected into the volume. This allows the catheter tip to be placed in the appropriate 3D position, with the knowledge that it is constrained to lie within a vessel that can be identified within the 3D model (Baert *et al* 2003).

9.2. MRI

OR-based MRI is one means of providing real-time imaging during a surgical procedure. In general, there have been three system designs for this purpose.

- Special purpose horizontal-bore 0.5 T superconducting magnet systems, designed exclusively for dedicated use in the operating room, have an open design that allows the surgeon minimally restricted access to the patient, and which permit imaging to take place during a surgical procedure.
- General-purpose 0.2 to 0.3 T permanent- or electro-magnet systems with open access to the patient from all sides.
- Conventional self-shielded 1.5 T horizontal bore systems with rapid fall-off of the fringe field.

All of these systems employ adaptations of conventional intra-operative tracking systems to follow the positions of probes and instruments in the operating field.

The first design employs a ‘double-donut’ superconducting magnet geometry that permits access to the patient between the two toroidal magnets (Black *et al* 1997, Schenck *et al* 1995) with sufficient space between the magnet sections for a surgeon to work. Most of the pioneering developments in their use has taken place at the Brigham and Women’s Hospital in Boston (Black *et al* 1997, Moriarty *et al* 1996).

The second approach is based on permanent, or electro-magnets which may be set up with their magnetic fields in either a horizontal (Hinks *et al* 1998) or a vertical (Steinmeier *et al* 1998, Tronnier *et al* 1996) configuration. These systems are usually general purpose low-field machines, whose inherent design makes them particularly suitable for use in the operating

room. Because of their design, they have almost no fringe field and are therefore much more amenable to the operating room environment than an air-cored superconducting magnet. While access is possible from all sides in the horizontal plane, the proximity of the pole-pieces restricts the access vertically to less than 40 cm. An early report by Steinmeier *et al* (1998) reported their initial experiences with this system. They used it to guide the surgical treatment of patients with supratentorial brain tumours, trans-sphenoidal operations and temporal lobe epilepsy procedures. They concluded that the intra-operative MR images obtained during these procedures provided considerable additional information that optimized the resection of tissue in these operations. More recently, a number of groups have reported on the use of a more user-friendly compact MRI device for neurosurgery guidance (the ODIN PoleStar®) (Schulder *et al* 2003). This low-field (0.12 T) system contains pole-pieces that are integrated with the OR table, and which can be raised when required so the patient's head occupies the space between the poles. Reports on its clinical utility indicate that it provides adequate real-time image-guidance in a number of surgical procedures, with the added advantage that it can be used in conjunction with standard neurosurgical tools (Kanner *et al* 2002).

The third means of using MRI intra-operatively is to adapt standard clinical MR imagers for operating room use by increasing the diameter of the bore and shortening the length of the magnet to improve access to the patient. At the same time the magnetic shielding must be sufficiently effective to permit the use of standard surgical tools and instruments (including x-ray image-intensifiers) in close proximity to the scanner (van Vaals 1998). A similar approach has been explored by Hoult *et al* (2001) who have developed a surgical magnet that is 'parked' adjacent to the operating room, but which is moved into the OR on ceiling mounted rails as required. Since this approach is based on a clinical magnet, access to the patient is not as convenient as in the previous two cases, and imaging is performed while the patient is placed inside the magnet between stages of the surgical procedure. On the other hand, this system exhibits the image quality expected from a standard diagnostic imaging system, and has been used successfully in a variety of neurosurgical procedures (Kelly *et al* 2005, Sutherland *et al* 2003). The next step in the development of this system is its integration with surgical robotics (Louw *et al* 2004).

Many of these systems permit imaging to occur during the surgical procedure itself, in some cases in real time using dynamic sequences. For the low-field open systems, the compromises that must be made to ensure increased access to the patient often degrade the linearity of the gradients across the field of view. For this reason, the geometrical integrity and resolution of images from such systems is often not as high as that available from conventional diagnostic MR systems. Nevertheless, the ability to visualize the target structures, and the surrounding anatomy in real time, offers a unique opportunity for image-guided surgery. Perhaps the most attractive feature of these devices is that the progress of certain therapies, e.g., cryo-surgery (Gilbert *et al* 1997, Klotz *et al* 1997b), thermal ablations (Chung and Sackier 1998, Chung *et al* 1997, Zhang *et al* 1998) and high-intensity focused ultrasound (HIFU) (Clement *et al* (2005)) can be monitored in real time by measuring changes in MR characteristics that are undergone by the tissues during freezing or heating. The major disadvantage of these devices is that even in the most 'open' of systems, access to the patient is not optimal, and the presence of the magnetic field in the operating room creates a potentially unsafe environment, unless instruments are modified for compatibility.

Intra-operative MR systems have now been evaluated clinically for at least a decade, and there is still much debate about the efficacy of these techniques in terms of cost effectiveness, improved patient outcome, image resolution and OR compatibility. While their proponents are extremely enthusiastic about their potential for widespread use, to date the adoption of this technology has been slow.

9.3. Computed tomography

CT scanners have existed in some operating rooms for many years. However, it has been only recently, through the provision of 'CT fluoroscopy' or 'fluoro CT' (Sakurai *et al* 2004, Solomon *et al* 2002) which scans and reconstructs a single plane repeatedly with updates approximately every 100–200 ms, that CT has been considered a true 'intra-operative' imaging device (Fichtinger *et al* 2004, Masamune *et al* 2001). A significant problem limiting the use of CT in the OR as an intra-operative imaging modality has been the radiation dose delivered to both patient and surgeon. Since it is not feasible to use an OR-based CT for routine diagnostic purposes as well, it is often difficult to justify the use of intra-operative CT economically. The former concern has stimulated the development of special-purpose robotic devices (Cleary *et al* 2005b) that can remotely manipulate instruments to access a target. Fichtinger *et al* (2004) describe a visualization environment that permits the CT fluoroscopic image containing the target to be virtually 'projected' via a semi-transparent mirror into the patient volume to guide manual biopsies.

A more recent incarnation of CT has evolved from C-arm based angiography machines. When appropriately calibrated (Fahrig and Holdsworth 2000), these systems can acquire high-resolution 3D images of organs in a single gantry rotation with an effective receptor resolution of $\sim$1000 $\times$ 1000 elements. When employed for vascular imaging these systems are often referred to as computed rotational angiography (CRA) or 3D reconstruction angiography. CRA has found application in the planning and guidance of surgical procedures for the treatment of intracranial aneurysms (Lauriola *et al* 2005), and arteriovenous malformations (Colombo *et al* 2003). In its non-angiographic manifestation this modality is commonly called cone-beam CT (CBCT), and is beginning to play a role in the guidance of non-vascular minimally-invasive procedures (Siewerdsen *et al* 2005).

9.4. Ultrasound

Ultrasound has been employed for many years as an interventional imaging modality (Auer and van Velthoven 1990). It is generally conceded that the image quality available from ultrasound is inferior to that attainable from even low-field intra-operative MRI (Steinmeier *et al* 1998), but ultrasound is being employed with increasing frequency as an intra-operative imaging device, either used alone or in registration with pre-operative image data sets. To combine intra-operative US with pre-operative MR images, the US images must be acquired in such a way that they can be mapped to the MR data. Trobaugh *et al* (1994) introduced the concept of correlating intra-operative US with pre-operative CT or MRI, and others have developed various techniques to either compare 2D ultrasound images to other modalities (Koivukangas *et al* 1993, Comeau *et al* 1998), or to accumulate a series of ultrasound images to create volumetric data sets (Rohling *et al* 1998, Downey *et al* 2000, Fisher *et al* 1998). Many techniques for acquiring and displaying 3D ultrasound data have recently been described in the literature and many have direct relevance to the acquisition of intra-operative 3D images. Given the expense of interventional MRI, intra-operative US is seen as a viable alternative for imaging tissue during surgery (Holm and Skjoldbye 1996, Machi and Sigel 1996). Besides detecting the changes that occur during surgery, US may also be used to update pre-operative images to match the changing intra-operative morphology.

Comeau *et al* (2000) proposed the identification of homologous landmarks within MRI and ultrasound images to construct a set of distortion vectors, which would allow the image of the pre-operative MR image to be warped to match the intra-operative MRI. They demonstrated the clinical utility of combining ultrasound images with pre-operative MRI's and the feasibility of

deforming the pre-operative MR slices to match the intra-operative US images. This work was subsequently extended to embrace the use of true 3D ultrasound image acquisition (Gobbi and Peters 2002, Hernes *et al* 2003, Kaspersen *et al* 2003b, Lindseth *et al* 2003). One disadvantage of intra-operative ultrasound compared to interventional MRI is that the ultrasound transducer must be in direct contact with the brain tissue during imaging, and its presence, along with the associated tracking mechanisms presents an intrusion into the operating field. A further disadvantage is that the image quality is somewhat operator dependent. In recent years, the integration of pre-operative images with intra-operative ultrasound has extended to the guidance of many procedures outside the brain. Although many of these procedures use conventional 2D US, 3D techniques are becoming increasingly available (Fenster *et al* 2001). 3D ultrasound has played a particularly important role in the guidance of prostate biopsy and brachytherapy (Blake *et al* 2000, Robb 2002, Wei *et al* 2004), where targets can be visualized and biopsy needles or radioactive seeds can be placed interactively within the 3D volume. Although precise visualization of inserted needles can be problematic in the raw US image, real-time image processing techniques can accurately extract the position of the needle tip. In recent years, laparoscopic ultrasound, either correlated with, or registered to pre-operative CT (Wilheim *et al* 2003, Kaspersen *et al* 2003a) has been reported as an adjunct to abdominal procedures. Kaspersen concludes that the integration of real-time intra-operative ultrasound with high quality pre-operative images permits increased identification accuracy of structures observed in the US images even if the registration accuracy (7–13 mm) is less than ideal. The key point is that such image integration provides the user with the proper context of the (often poorly resolved and noisy) US images.

10. Display systems

An important component of an IGS system is the display. It must be capable of presenting the image in three dimensions, either by displaying orthogonal planes that follow the position of the tracked probe, or by displaying the probe within a three-dimensional rendition of the patient volume of interest. To be an effective tool in the OR, the display must be truly interactive. Many research and commercial workstations are available to perform a variety of operations on medical images, but there are several worthy of special mention. Analyze (Robb *et al* 1989, Robb 1999), a package that grew out of the Biomedical Imaging Resource at the Mayo Clinic, Rochester MN, is probably the longest surviving such package, and served to bring together tools for generalized manipulation, measurement and visualization of multi-dimensional medical images in a user-friendly environment. Another more recent package, that has found application in many laboratories, is 3D-Slicer (Gering *et al* 2001), from The Brigham and Women's Hospital/MIT. The latter package has embraced the 'open-source' philosophy, itself making extensive use of open-source libraries such as VTK (Schroeder *et al* 2000) and ITK (Yoo and Ackerman 2005).

10.1. Multi-planar imaging

The representation of image volumes in a multi-planar reformatted (MPR) mode is as old as CT image acquisition itself, and even in the presence of volumes whose voxels were far from isotropic (with voxel dimensions typically $1.5 \times 1.5 \times 13\ \text{mm}^3$), MPR was useful in navigating through the images in three dimensions. Today, isotropic data acquisition is possible with both CT and MRI, and voxel dimensions can be smaller than $1\ \text{mm}^3$. Early computer systems were only capable of slicing the data along orthogonal axes (rows and columns). Today's systems

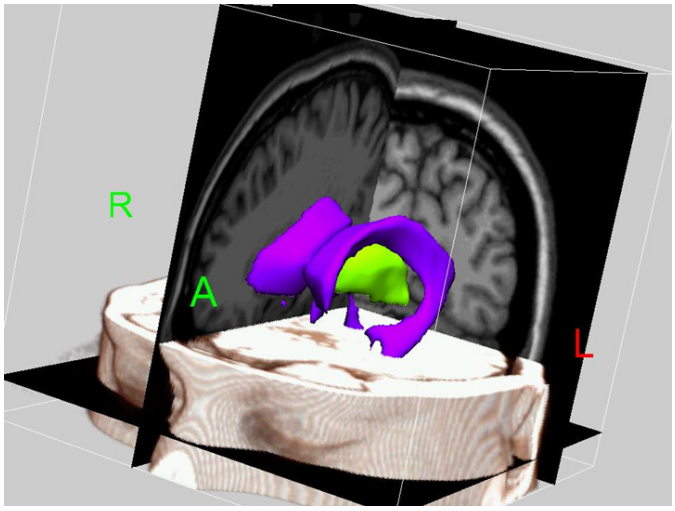

Figure 5. Stereotactic neurosurgery planning and guidance display incorporating surface rendering (Corpus callosum, thalamus), texture-mapped (original MRI data on orthogonal planes) and volume rendered (head surface) data in the same image.

permit the interactive selection of arbitrary slices from the volume, allowing the user to select views that are perpendicular to the direction, or in the plane of the probe, as well as any other views that are appropriate for the procedure.

10.2. Three-dimensional visualization

The traditional means of displaying medical images was using an x-ray film on a view-box, and even after CT and MRI were introduced, image volumes were still viewed slice-by-slice, either as films on a standard light box, or on a computer display. As the volume of data in a typical image increased, it became necessary to display the image as a single entity, rather than as a collection of slices. The display of these data (volumes of voxels) may be achieved either by projecting surfaces within the volume (Lorensen and Cline 1987), or projecting the entire volume onto a viewing screen (Drebin *et al* 1988, Levoy 1988). These two approaches are known as surface rendering and volume rendering, respectively.

Surface rendering, the most common method of displaying 3D medical images, requires that the volume be segmented (by automatic or manual contouring methods) (Saiviroonporn *et al* 1998, Soler *et al* 2001) so the surfaces of structures of interest are identified within the volume. Surface rendering is often used in conjunction with texture-mapping to 'paint' characteristics of the original data (voxels) onto selected surfaces within the 3D images (Lorensen and Cline 1987). An example of a combined surface/texture-map display is given in figure 5. In contrast, volume-rendering employs direct or simulated ray-tracing techniques (Radetzky *et al* 2000) where the intensity of each point in the projected image is a function (line integral, maximum intensity, etc) of the structure traversed by each ray. In either case, contemporary computer workstations are sufficiently powerful to allow interactive manipulation of either kind of image, although special hardware on graphics processing units is often employed to accommodate the computational demands of volume rendering algorithms.

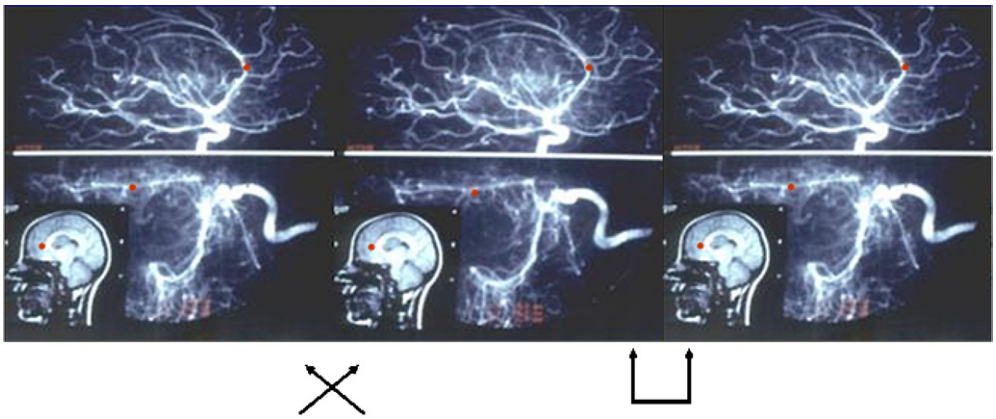

Figure 6. Multi-modality stereotactic stereoscopic planning display. A-P and lateral DSA images are displayed along with a sagittal image of the patient's MR study. Target points are indicated in the angiogram in red, and those that fall within the displayed MR image are indicated as well. The left pair of images is designed for cross-eye viewing, while the right pair can be viewed with wall-eye (relaxed) viewing.

10.3. Stereoscopic visualization

Stereoscopic imaging is no longer in general use in diagnostic radiology, although there are some centres that still employ it routinely, while others do so on a sporadic basis. Since the advent of three-dimensional imaging modalities, there is an increased need to navigate through large data spaces quickly. The use of 3D visualization in surgical planning and guidance and the availability of inexpensive computational power that permits the interactive manipulation of three-dimensional volumes has once again made stereoscopic visualization (George *et al* 2002) a compelling adjunct to surgical navigation, particularly within virtual immersive environments. Stereoscopic visualization has been employed in the operating room by the surgical team at the Montreal Neurological Institute (MNI) for a number of years, initially for the integration of digital subtraction angiograms with MRI and CT for surgical planning purposes (Charland and Peters 1996, Peters *et al* 1994, Worthington *et al* 1985). Figure 7 presents an example of stereoscopic DSA images typical of those used when planning stereotactic surgical implantation of deep brain electrodes prior to surgery for epilepsy. The use of stereoscopic visualization in modern surgical guidance systems is further discussed later in this review. Subsequently, the MNI group incorporated stereoscopic visualization into the three-dimensional views presented to the surgeon during surgical guidance, displaying dynamic representations of the surgical probe along with surfaces and MRI slice data (Davey *et al* 1994, Peters *et al* 1996). More recently, they extended the use of stereoscopic visualization to the planning of thalamotomies and pallidotomies for the treatment of Parkinson's disease. In this area, stereoscopic visualization has proved to be a major advantage when planning the shape and position of a three-dimensional lesion that must be placed precisely with respect to a functional atlas that has been merged with the data (St-Jean *et al* 1998).

The advantages of stereoscopic visualization in the surgical planning and guidance context have been debated for decades. While it has proved valuable in the neurosurgical procedures discussed above, its use as a dexterity improving aid for laparoscopically guided techniques (suturing, knot-tying, etc) is less clear. However, Munz *et al* (2004) recently demonstrated

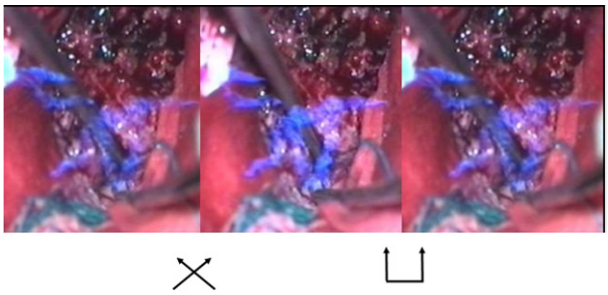

(a)

(b)

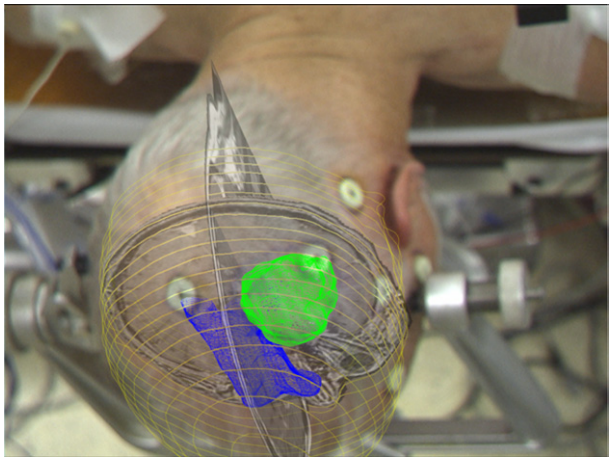

(c)

Figure 7. Augmented reality visualization. (a) Merged data from a tracked microscope and computer model of vascular structures (derived from pre-operative images), lying beneath the surface. Displayed for stereoscopic viewing as for figure 6. (Images courtesy Dr David Hawkes, University College London). (b) Pilot test of the Siemens Corporate Research (SCR) AR system at the Hospital of University of Pennsylvania. 3D fused image of tumour inside the head. (c) Image as seen by the operator wearing the head-mounted display. Images courtesy of Dr Frank Sauer, SCR.

that stereoscopic visualization consistently and significantly improved performance for a number of common manoeuvres in robot-assisted surgery. It should be pointed out that these tests related to direct (endoscopic) stereo vision, and the system was not complemented by augmented reality.

10.4. Virtual and augmented reality

In a strict sense, virtual reality applies to any kind of environment where an image is employed to model an organ and/or to guide an instrument to the organ. In this review its scope is limited to the presentation of 3D models that can be manipulated dynamically and which are generally displayed to the observer stereoscopically. In addition, augmented reality (Drasic and Milgram 1996) refers to the situation where 'real-world' images (video, endoscopic, ultrasound, or even electrophysiological) are integrated with the visualized model. In addition to the incorporation of video images acquired during the surgical procedure, there exist a number of other approaches for combining the real and modelled worlds into a common visualization framework.

Video information can add a great deal of information to an image-guided surgical procedure. Gleason *et al* (1994) were the first to demonstrate the efficacy of integrating a video image of the operative site with the graphical representation of a tumour or other target structure. This approach enables the surgeon to 'see-through' the patient's skin into the operative site, and can facilitate the planning of the optimal craniotomy required to approach the target.

Since many surgical procedures involve the use of an operating microscope, the integration of the microscope images with those obtained from pre-operative MRI and CT scans is an obvious step. Image integration can involve displaying the position of the focal point of the microscope within the 3D image, or images from a tracked microscope can be integrated electronically with the pre-operative images. Alternatively, the images from the pre-operative scans can be projected into the visual field of the microscope (Edwards *et al* 1995, Edwards *et al* 2000) (figure 7). This same technology has also been incorporated into head-mounted displays where the position of the surgeon wearing such a display is tracked and the pre-operative image corresponding to the viewpoint of the surgeon is projected on his field of view (Figl *et al* 2002, Levy *et al* 1998, Vogt *et al* 2004).

Operating microscopes 'see' into a surgical target within the brain via a craniotomy of at least 2 cm in diameter. For minimally-invasive procedures, an endoscope must be employed instead. Endoscopes are used to gain visual access to body cavities, and have been employed in neurosurgery to assist in surgical procedures within the ventricles (Auer *et al* 1988). 'Virtual endoscopy' (Auer and Auer 1998, Gilani *et al* 1997, Vining 1996) uses computer graphics to simulate the view of an endoscope placed in a particular body cavity, based on the representation of the cavity derived from pre-operative MRI or CT images. With the increasing emphasis on minimally invasive surgery, there has been an active interest in combining the video images from standard endoscopy with the computer-generated images of virtual endoscopy. The aim is to place the endoscope image observed during a minimally invasive surgical procedure in its proper context, by merging it with the equivalent surface extracted from the pre-operative images. Several authors have reported their experiences with clinical applications whereby images of the ventricle wall obtained from a tracked endoscope were combined with the equivalent images from CT or MRI (Auer and Auer 1998, Shahidi *et al* 1995, 2002, Stefansic *et al* 1998). The simplest means of integrating the two modalities is to track the tip of the endoscope, while displaying the tracked point on three orthogonal slices from the original image data that intersect at the tracked point. While useful, this

approach does not present the endoscopic image in its proper context. To achieve this latter aim, the video image produced by the endoscope may be mapped onto an interior surface model explored by the endoscope (Dey *et al* 2002). A similar approach has been described by Szpala *et al* (2005) for registering endoscopic images with pre-operatively acquired dynamic models of the beating heart.

Such environments can be employed both at the planning stage of a procedure (George *et al* 2002, Mastrangelo *et al* 2002) where surface and volume rendered CT data are viewed during the planning of a laparoscopic procedure, or during the operation itself. Recently, a number of novel approaches for combining model information with 'live' images have been proposed. These generally fall into three distinct classes, those employing microscopes; systems using head-mounted displays (HMD's); and those that rely on mirrors, which reflect a virtual image into the operating volume. In a microscope-based system, a binocular microscopic image is optically merged with a stereoscopic image generated from a model after ensuring that the model viewing geometry precisely matches that of the optical imaging system, as demonstrated by Edwards *et al* (1995, 1999, 2000). This group has also demonstrated that merging stereo images of real and virtual scenes can sometimes lead to ambiguous depth assessment (Johnson *et al* 2003), clearly indicating that there remains a great deal of work to understand how the human visual system behaves when interpreting such displays. Head-mounted displays can fuse the virtual model with the direct view (as in the microscope) (Birkfellner *et al* 2003a, 2002, Figl *et al* 2005), or electronically combine both the model and camera views (Vogt *et al* 2004). In both of these cases, head motion is tracked and used by the model generation software to generate the appropriate view of the model regardless of the pose of the observer. A compelling approach that does not require any head-tracking is described by Blackwell *et al* (2000) and Fichtinger *et al* (2004). These systems use a semi-transparent mirror to project a virtual image of a body section obtained from CT or MR directly into the volume containing the organ under consideration. Although only a single user-selected slice can be displayed, a properly calibrated system places this slice correctly regardless of the position of the viewer. A similar concept is employed by Stetten *et al* (2003), in the 'sonic flashlight' where the real-time ultrasound image is reflected by a simple semi-transparent mirror into precisely the region from which the ultrasound images are being acquired.

Perhaps the most interesting (also the most expensive) approach to this problem is that proposed by Liao *et al* (2003, 2004a, 2004b) where an array of video projectors and a large 'fly's eye' lens are used to generate a three-dimensional virtual image that can be projected (again using a half-silvered mirror) into the patient volume. Because of the true 3D nature of the virtual image created by this approach (i.e. it is not the result of a stereo pair from a single viewpoint), this image is also viewable by multiple observers without head tracking.

A full discussion of virtual reality in medicine is given by Englmeier (2000).

11. Robotics

In the past few years, robotics have played an increasingly important role in minimally-invasive surgical procedures. An early significant application was in the surgical implantation of hip prostheses into the femoral canal, using 'Robodoc' as introduced by Paul *et al* (1992). Their objective was to use image-directed surgical robotics to precisely ream the femoral canal to obtain an exact match with the prosthesis. The major breakthrough in this field was that the prosthesis shaft could be constructed precisely according the geometry of the femur as

determined from 3D CT scans, then the robot was employed to manipulate the implant into its final position. Paul's work found that the in-growth process is facilitated when the surgeon achieves a tight fit for the prosthesis over the length of its shaft.

Sawaya *et al* (1995) speculated on the possibilities of using robotically assisted procedures and virtual reality to improve tumour surgery, while Benabid *et al* (1995) published an excellent review on (neuro)surgical robotics, discussing many of the early contributors, including the pioneering work of Kwoh *et al* (1985) and Kwoh and Young (1992). Benabid discusses the use of robots to position instruments in a stereotactic setting, and also describes later implementations of this concept in other centres using commercially available robotic arms.

One commercial implementation of these ideas is the neurosurgical operative microscope as described by Giorgi *et al* (1995). Here a robotic arm is connected to a microscope, while force feedback sensors drive the motors of the arm in response to the positioning of the microscope by the surgeon. The coordinates of the microscope focal point (and potentially the images acquired by the microscope optics) are integrated with the standard multi-planar and 3D MRI views of the patient on the surgical workstation. Chen *et al* (1998) describe a prototype system that incorporates pre-operative image-guided planning, minimally-invasive and non-invasive calibration between the virtual (patient images) and actual environment, and a surgical robot for location and remote-controlled procedures based on the pre-operative strategy.

The past decade has seen a resurgence in the use of robotics in surgery to improve the precision and dexterity of minimally-invasive procedures. At the present time, however, little effort has been expended on integrating pre-operative imaging with robotics, with modern robotic surgery being 'image-guided' only in the sense that it generally employs a robotically-manipulated endoscope that captures the view of the target and the instruments. Medical robotics have been used extensively in coronary artery bypass grafting (CABG) (Falk *et al* 2003, Novick *et al* 2003). Beyond the heart, it has been claimed that such techniques can be combined with imaging to dramatically increase the precision of paediatric surgery (Kant *et al* 2004). Hemal and Menon (2004) reviewed the application of robotically-assisted procedures in urology, concluding that significant initial promise is being shown for radical prostatectomy, while Ballantyne and Moll (2003) discuss the role of robotics in telesurgery environments. While few of these applications rely explicitly on guidance from images other than from the endoscope, a group from INRIA (Coste-Maniére *et al* 2003a, 2003b) describe the most compelling use of pre-operative imaging with robotics, integrating image-based models with robotic systems to plan effective strategies for performing CABG procedures.

It is clear that for the most part, special-purpose robotic tools designed to perform specific tasks are preferred over general purpose systems for minimally-invasive procedures. In this light, Cleary *et al* (2005a) have described the use of a special purpose robot to drive a biopsy needle to a target under the guidance of CT fluoroscopy. In addition, the CISST group at Johns Hopkins University (Burschka *et al* 2005) recently discussed the challenges involved in image reconstruction, instrument tracking and registration as they relate to robotically-assisted minimally invasive surgery, as well as the integration of these techniques into realistically achievable, practical and reliable systems. Several workshops have recently addressed the role of robotics in medicine. At one of these (Cleary *et al* 2005b), the participants concluded that although several medical robot manufacturers had already gone out of business, there remained a great deal of optimism in the future of robotically-assisted procedures. A second workshop (Cleary 2005c) speculated on the nature of the operating room in the year 2020 and resulted in a comprehensive report on the current status of robotics and imaging in surgery.

Figure 8. Typical image-guidance environment in the operating room. Note the disconnect between the operating field at the tip of the tracked probe, and the view on the display monitor.

12. Operating room environment

Given the huge range of technology available for image-guided surgery, it should be noted that it must all fit physically and be functional within the operating room. Figure 8 shows a view of the surgical team employing a tracked probe during an image-guided neurosurgery procedure. One of the first points to note is how far the image monitor is located from the surgeon. This is typical, and is dictated by the bulk of the equipment and the generally confined space in the OR. Unfortunately, this does not provide the ideal ergonomic environment for the surgeon who must constantly move his head and re-accommodate his vision each time he looks between the monitor and the surgical field. The situation can be improved by placing a flat-panel display close to the operating field. The tracking system attached to the probe shown in figure 8 is optical, and although it is light-weight, it suffers from 'line-of-sight' constraints, and ceases to operate when the LED emitters lose sight of the tracking device.

13. Image acquisition caveats

Imaging systems designed specifically for diagnostic purposes are not necessarily optimal for surgical guidance, which relies on images being accurate geometrical representations of the organs of interest. The discussion below summarizes some of the important attributes of imaging systems related to their use in image-guided surgery.

13.1. CT

The standard CT image is intrinsically geometrically accurate, but errors in patient or gantry alignment can result in errors in relating image coordinates to world coordinates. For example, if the slices are oblique to the scanner axis, but reconstruction software assumes them to be perpendicular, the resulting three-dimensional reconstruction will be distorted. Likewise, variable slice thickness and positioning can create geometrically distorted volumes

if image-processing software does not account for arbitrary sampling of the imaging volume. Fortunately, the recent adoption of CT scanners capable of acquiring up to 64 simultaneous slices has removed many of the issues related to non-isotropic image resolution and slice alignment.

13.2. MRI

When MRI arrived on the scene, certain metallic components of stereotactic frames that could be imaged with CT or radiography without problems, had to be replaced by non-metallic components to avoid creating magnetic field perturbations that would distort the images. Likewise, copper or aluminium fiducial markers must be replaced by channels in plastic plates filled with a fluid that produces a bright signal in an MR image (Lunsford 1988). If these channels are filled with water-based, x-ray contrast agent, the fiducial markers are visible in MRI as well as CT. From time to time, oil has been suggested as a suitable fluid for use in MR fiducial markers, but since the resonant frequency of oil-based protons is 200 ppm different from free water, this approach is impractical, since the fiducial markers in the MR images may be shifted from their true positions by several pixels.

The most probable causes of image distortion in MRI are that the main magnetic field lacks homogeneity across the volume of interest, that the gradients have spatial nonlinearities, or that the magnetic field is perturbed locally by the presence of either an internal or external influence. Even very small deviations of the field strength (tens of parts per million) from the ideal can have a significant impact on the geometrical integrity of the images, and the effect of gradient nonlinearities tends to be particularly noticeable towards the periphery of the field of view.

An additional factor that distorts the image is the effect of material having a magnetic susceptibility different from human tissue. Such susceptibility differences cause small local changes in the magnetic fields, which again can create distortions in the images. Examples of this phenomenon are the presence of dental work or metallic prostheses near the imaging field (such objects can render the image completely useless) or the susceptibility difference between air/water/bone which can cause image distortions close to the material interfaces.

Unless the main magnetic field inhomogeneity has been caused by gross failure of the (usually super-cooled) electromagnet windings, homogeneity corrections can be made to the main field using shimming techniques. This can either be in the form of active shims (additional nonlinear gradient coils that provide controllable field patterns added to the main field to counter imperfections), or passive shims (iron inserts that are placed in specified patterns inside the magnet bore to modify the global field pattern with the influence of their induced magnetic fields). Many installed MR imagers equipped with active shims have calibration procedures that allow the shim fields to be adjusted to maximize main field uniformity across the field of view.

Distortions due to gradient design limitations are often corrected automatically (at least in the plane of the image) by the scanner software. Where this facility is available, it should be determined that the applied correction software has been invoked, and that the correction is appropriate for the imaging sequence.

Non-uniform radio-frequency excitation can cause inhomogeneous intensity distributions in the reconstructed images. While image non-uniformities may not affect the diagnostic utility of the images, they can significantly impact quantitative image analysis, for example when segmentation is performed using an intensity threshold. Unless corrected, such intensity artefacts can severely compromise the integrity of surface extraction, in turn reducing the quality of the image registration and the accuracy of the segmentations. RF non-uniformity

correction schemes are not normally included in the MR image reconstruction process, but there are numerous approaches that may be employed retrospectively to restore the correct image intensities (Arnold *et al* 2001, Belaroussi *et al* 2006)

13.3. Ultrasound

Although ultrasound is inexpensive and unobtrusive, it has its own limitations. One immediate obstacle to its use in some circumstances is that intimate contact between the transducer and the tissue must be maintained at all times, usually via a water or gel acoustic matching medium. Since the US signal relies on reflection from impedance interfaces in the medium, a large impedance mismatch causes strong reflections and consequently low forward transmission of the US energy. Consequently, US does not propagate past pockets of gas or bony structures. In addition, US systems are calibrated to assume a sonic transmission speed of 1540 m s^{-1}, the mean velocity of sound in soft tissue. However, if the propagation velocity is different from this (e.g. fat at $\sim$1475 m s^{-1}), significant image distortion may result. An additional limitation of US is that its resolving capability is inhomogeneous across its field of view, with the slice varying in thickness throughout the field of view. Also the axial resolution is typically significantly better than the lateral, and both axial resolution and the depth of field are functions of the wavelength of the US wave, with depth of penetration being traded for increased resolution.

14. Conclusions

In the operating room of the future, perhaps the greatest challenge to the successful adoption of image-guided surgery systems relates not to technology, but to the user interface. Over the past several years, affordable high-speed computing hardware has become available that allows interactive surgical image-guidance to be performed in real time with stereoscopic visualization. So far, little effort has been expended to ensure that the human factors issues relating to the use of such equipment in the OR have been adequately addressed. The key will be to design these systems so they are unobtrusive and simple to operate. The logistics of data management (acquisition of images, merging them with scans from other sources and segmenting the relevant structures) must be handled either automatically, or with a minimum of intervention. It ultimately must be possible to operate computer systems in the OR without the use of a keyboard or complicated switching devices. The IGS system must not add time or complication to the procedure.

It might be argued that IGNS will have a significant impact on ‘difficult’ procedures that could not be performed satisfactorily, if at all, without computerized image-guidance. It is probable, however, that it will have the greatest overall effect when it becomes a standard operating-room tool for routine procedures, reducing OR time, decreasing patient trauma and streamlining data management. The effective integration of this technology with hospital information systems will play a significant role in its widespread acceptance.

The psychophysical issues of manipulating objects within a virtual 3D environment have barely been addressed to date. Today’s technology provides us with a wealth of tools (VR displays, high-speed interaction, haptic feedback, etc), but without a detailed understanding of how the human visual/sensory system interacts with these tools, their advantages may be lost.

The recent workshop entitled ‘OR2020—The Operating Room of the Future’ (Cleary 2005c) identified the state of the art in many areas relating to the future directions of surgical practice. One chapter of the resulting proceedings, devoted to ‘Imaging in the Operating

Room', defines a number of imaging-related roadblocks to overcome and lists critical research priorities to further advance minimally-invasive surgical procedures.

The participants of this workshop deemed the quality of current intra-operative imaging techniques to be poor, and it was noted that PACS systems (designed for the diagnostic radiologist) available in the OR rarely have 3D visualization capability, instead simply reproducing the standard 'view-box' format of the conventional radiology viewing room. Unless this situation changes, PACS systems cannot meet the demands of the surgeon in the OR.

All relevant patient images must be tracked within a database so that they can be immediately recalled, made available to the surgeon at the time of operation, and directly correlated with intra-operative images. One of the key components of image-guided surgery, and arguably its most important aspect, is the ability to track instruments in the surgical field and to register them to images and the patient. There are no current standards in this area, and standardization of universal imaging and registration methodologies will be key to the development of new navigational systems.

Segmentation is an important part of intra-operative image utilization, to extract surface information, to facilitate image registration, and to provide realistic organ visualization during the procedure. Segmentation is not typically provided by most commercial visualization packages, perhaps because it falls into the category of 'tampering with the data', in the sense that any rule applied to an image to define a surface will inevitably compromise the data to some extent. The increasing speed of ray-casting algorithms may alleviate this problem somewhat by providing interactive volume visualization without the need for *a priori* segmentation. Since universal segmentation algorithms are unlikely ever to become entirely automatic, there is a need for intuitive interfaces to permit human intervention in the selection of the desired region, as well as evaluating the consistency of the results.

The following research priorities were identified as being crucial for further development of intra-operative image-guidance.

- Development of targeted imaging integration systems, incorporating integrated displays that allow multiple imaging modalities to be visualized simultaneously. These systems must incorporate integrated tracking and registration across modalities, across tools and other equipment so that all data are inherently registered to a single, common coordinate system.
- Development of advanced registration techniques to integrate pre-operative imaging with 3D real-time intra-operative imaging, along with techniques to effectively measure the errors encountered in rigid and non-rigid image registration.
- New imaging systems must be designed from the ground up, based on the requirements of the OR instead of bringing current/traditional radiology systems into the OR.
- Future surgical procedures for which image-guidance will be appropriate, along with the imaging modalities that will be necessary, need to be identified. While it is likely that new advances such as molecular imaging could well change the kind of surgeries and treatments that are practised in the future, present imaging modalities need to be considered as the building blocks upon which future developments will be based.
- The value of intra-operative imaging must be established by the implementation of appropriate standards to permit the medical community to objectively assess the efficacy of various imaging and guidance strategies.

Image-guided surgery has had a rich history, and has made significant contributions to healthcare, particularly in neuro- and orthopaedic surgery. As image acquisition and information technology has advanced, we have the potential to develop new approaches to

surgical and therapeutic problems that go beyond simply 'fine tuning' existing techniques. Many challenges remain, but continued multidisciplinary and multi-institutional research efforts, along with the ever increasing improvements to imaging and computer technology, will finally enable most interventions to be accomplished without the need to subject the patient to 'surgery'.

Acknowledgments

I would like to thank the Editor of PMB for inviting and encouraging me to write this review. I also wish to acknowledge my graduate students, fellows and colleagues over the years for the contributions and insight they have provided to this field. I am also indebted to Jackie Williams who has provided valuable editorial support in writing this review. Support for my work in image-guided surgery has been provided by the Canadian Institutes for Health Research, the National Science and Engineering Research Council of Canada, the Ontario Heart and Stroke Foundation, the Canadian Foundation for Innovation, the Ontario Research and Development Challenge Fund, and the Institute for Robotics and Intelligent Systems. This review builds on previous work published by the author in chapter 3: 'Image-guided surgery', of the SPIE Medical Imaging Handbook, vol 2: Image Display and PACS. SPIE Press, 2000, and in 'Image-guided surgery: from X-rays to Virtual Reality', Computer Methods in Biomedical Engineering, **4**(1) 27–57, 2000.

References

Alterman R L, Kall B A, Cohen H and Kelly P J 1995 Stereotactic ventrolateral thalamotomy: is ventriculography necessary? *Neurosurgery* **37** 717–21

Appelbaum L, Lederman R, Agid R and Libson E 2005 Hepatic lymphoma: an imaging approach with emphasis on image-guided needle biopsy *Isr. Med. Assoc. J.* **7** 19–22

Arnold J B, Liow J S, Schaper K A, Stern J J, Sled J G, Shattuck D W, Worth A J, Cohen M S, Leahy R M, Mazziotta J C and Rottenberg D A 2001 Qualitative and quantitative evaluation of six algorithms for correcting intensity nonuniformity effects *Neuroimage* **13** 931–43

Audette M A, Ferrie F P and Peters T M 2000 An algorithmic overview of surface registration techniques for medical imaging *Med. Image Anal.* **4** 201–17

Auer L M and Auer D P 1998 Virtual endoscopy for planning and simulation of minimally invasive neurosurgery *Neurosurgery* **43** 529–48

Auer L M and van Velthoven V 1990 *Intraoperative Ultrasound Imaging in Neurosurgery: Comparison with CT and MRI* (New York: Springer)

Auer L M, Holzer P, Ascher P W and Heppner F 1988 Endoscopic neurosurgery *Acta Neurochir.* **90** 1–14

Baert S A, van Walsum T and Niessen W J 2004 Endpoint localization in guide wire tracking during endovascular interventions *Acad. Radiol.* **10** 1424–32

Baert S A, van de Kraats E B, van W T, Viergever M A and Niessen W J 2003 Three-dimensional guide-wire reconstruction from biplane image sequences for integrated display in 3-D vasculature *IEEE Trans. Med. Imaging* **22** 1252–8

Ballantyne G H and Moll F 2003 The da Vinci telerobotic surgical system: the virtual operative field and telepresence surgery *Surg. Clin. North Am.* **83** 1293–304

Belaroussi B, Milles J, Carme S, Zhu Y M and Benoit-Cattin H 2006 Intensity non-uniformity correction in MRI: existing methods and their validation *Med. Image Anal.* **10** 234–46

Benabid A L, Hoffman D, Munari C and Le Bas J F 1995 Surgical robotics *Minimally Invasive Techniques in Neurosurgery* ed A R Cohen and S J Haines (Baltimore, MD: Williams & Wilkins) pp 85–97

Bergstrom M and Greitz T 1976 Stereotaxic computed tomography *Am. J. Roentgenol.* **127** 167–70

Bertrand G, Olivier A and Thompson C J 1974 Computer display of stereotaxic brain maps and probe tracts *Acta Neurochirurg. (Suppl.)* **21** 235–43

Birkfellner W *et al* 2002 A head-mounted operating binocular for augmented reality visualization in medicine—design and initial evaluation *IEEE Trans. Med. Imaging* **21** 991–7

Birkfellner W, Figl M, Matula C, Hummel J, Hanel R, Imhof H, Wanschitz F, Wagner A, Watzinger F and Bergmann H 2003a Computer-enhanced stereoscopic vision in a head-mounted operating binocular *Phys. Med. Biol.* **48** N49–N57

Birkfellner W, Seemann R, Figl M, Hummel J, Ede C, Homolka P, Yang X, Niederer P and Bergmann H 2005 Wobbled splatting—a fast perspective volume rendering method for simulation of x-ray images from CT *Phys. Med. Biol.* **50** N73–N84

Birkfellner W, Watzinger F, Wanschitz F, Enislidis G, Kollmann C, Rafolt D, Nowotny R, Ewers R and Bergmann H 1998a Systematic distortions in magnetic position digitizers *Med. Phys.* **25** 2242–8

Birkfellner W, Watzinger F, Wanschitz F, Ewers R and Bergmann H 1998b Calibration of tracking systems in a surgical environment *IEEE Trans. Med. Imaging* 737–42

Birkfellner W, Wirth J, Burgstaller W, Baumann B, Staedele H, Hammer B, Gellrich N C, Jacob A L, Regazzoni P and Messmer P 2003b A faster method for 3D/2D medical image registration-a simulation study *Phys. Med. Biol.* **48** 2665–79

Black P M, Moriarty T, Alexander E, Stieg P, Woodard E J, Gleason P L, Martin C H, Kikinis R, Schwartz R B and Jolesz F A 1997 Development and implementation of intraoperative magnetic resonance imaging and its neurosurgical applications *Neurosurgery* **41** 831–42

Blackwell M, Nikou C, DiGioia A M and Kanade T 2000 An image overlay system for medical data visualization *Med. Image Anal.* **4** 67–72

Blake C C, Elliot T L, Slomka P J, Downey D B and Fenster A 2000 Variability and accuracy of measurements of prostate brachytherapy seed position in vitro using three-dimensional ultrasound: an intra- and inter-observer study *Med. Phys.* **27** 2788–95

Brown R A 1979 A computerized tomography-computer graphics approach to stereotaxic localization *J. Neurosurg.* **50** 715–20

Burschka D *et al* 2005 Navigating inner space: 3-D assistance for minimally invasive surgery *Robot. Auton. Syst.* **52** 5–26

Carrillo A, Duerk J L, Lewin J S and Wilson D L 2000 Semiautomatic 3-D image registration as applied to interventional MRI liver cancer treatment *IEEE Trans. Med. Imaging* **19** 175–85

Cash D M, Sinha T K, Chapman W C, Terawaki H, Dawant B M, Galloway R L and Miga M I 2003 Incorporation of a laser range scanner into image-guided liver surgery: surface acquisition, registration, and tracking *Med. Phys.* **30** 1671–82

Charland P and Peters T M 1996 Optimal display conditions for quantitative analysis of stereoscopic cerebral angiograms *IEEE Trans. Med. Imaging* **15** 648–56

Chen M D, Wang T, Zhang Q X, Zhang Y and Tian Z M 1998 Robotics system for stereotactic neurosurgery and its clinical application *IEEE Int. Conf. on Robotics and Automation* (Piscataway, NJ: IEEE) pp 995–1000

Chung Y C, Duerk J L and Lewin J S 1997 Generation and observation of radio frequency thermal lesion ablation for interventional magnetic resonance imaging *Invest. Radiol.* **32** 466–74

Chung J Y and Sackier J M 1998 A method of objectively evaluating improvements in laparoscopic skills *Surg. Endosc.* **12** 1111–6

Claron Technologies 2005 Claron Technologies Micron Tracker. http://www.clarontech.com

Cleary K 2005c *Operating Room of 2020 Workshop Report* http://www.or2020.org

Cleary K *et al* 2005a Precision placement of instruments for minimally invasive procedures using a 'needle driver' robot *Int. J. Med. Robot. Comput. Assist. Surg.* **1** 40–7

Cleary K, Davies B, Fichtinger G, Troccaz J, Leuth T and Watson V 2005b Medical robotics workshop—WRWS *Comput. Aided Surg.* **9** 167–70

Clement G T, White P J, King R L, McDonald N and Hynynen K 2005 A magnetic resonance imaging-compatible large scale array for trans-skull ultrasound surgery and therapy *J. Ultrasound in Med.* **24** 1117–25

Clifford M A, Banovac F, Levy E and Cleary K 2002 Assessment of hepatic motion secondary to respiration for computer assisted interventions *Comput. Aided Surg.* **7** 291–9

Clunie D 2006 DICOM Standard Status. http://www.dclunie.com/dicom-status/status.html

Collins D L, Holmes C J, Peters T M and Evans A C 1995 Automatic 3-D model-based neuroanatomical segmentation *Hum. Brain Mapp.* **3** 190–208

Colombo F, Cavedon C, Francescon P, Casentini L, Fornezza U, Castellan L, Causin F and Perini S 2003 Three-dimensional angiography for radiosurgical treatment planning for arteriovenous malformations *J. Neurosurg.* **98** 536–43

Comeau R M, Fenster A and Peters T M 1998 Intra-operative ultrasound imaging in image-guided neurosurgery *Radiographics* **18** 1019–27

Comeau R M, Sadikot A F, Fenster A and Peters T M 2000 Intraoperative ultrasound for guidance and tissue shift correction in image-guided neurosurgery *Med. Phys.* **27** 787–800

Coste-Maniere E, Adhami L, Antiphon P and Abbou C C 2003a Preparedness in robotically assisted interventions *Curr. Urol. Rep.* **4** 101–8

Coste-Maniere E, Adhami L, Mourgues F and Carpentier A 2003b Planning, simulation, and augmented reality for robotic cardiac procedures: the STARS system of the ChIR team *Semin. Thorac. Cardiovasc. Surg.* **15** 141–56

Cox J 1896 *Montreal Med. J.* **24** 661–5

Crum W R, Griffin L D, Hill D L and Hawkes D J 2003 Zen and the art of medical image registration: correspondence, homology, and quality *Neuroimage* **20** 1425–37

Crum W R, Hartkens T and Hill D L 2004 Non-rigid image registration: theory and practice *Br. J. Radiol. Spec.* **77** S140–53

D'Haese P F, Cetinkaya E, Kao C, Fitzpatrick J M, Konrad P E and Dawant B M 2004 Toward the creation of an electrophysiological atlas for the pre-operative planning and intra-operative guidance of deep brain stimulators (DBS) implantation *Proc. MICCAI 2004, LNCS 3216 (Heidelberg/France: Springer (D-69121), Saint-Malo)* pp 729–36

Dam H J W 1896 The new marvel in photography *McLure's Mag.* **6** 403

Danisch L A, Englehart K and Trivett T 1999 Spatially continuous six degree of freedom position and orientation sensor *Proc. SPIE 3541: Fiber Optic and Laser Sensors and Applications SPIE* (Bellingham, WA: The International Society for Optical Engineering) pp 48–56

Davey B L K, Comeau R M, Munger P, Pisani L, Lacert D, Olivier A and Peters T M 1994 Multimodality interactive stereoscopic image-guided neurosurgery *Proc. Visualization in Biomedical Computing* ed R A Robb (Bellingham WA: SPIE) pp 526–36

Dey D, Gobbi D G, Surry K J, Slomka P and Peters T M 2002 Fusion of endoscopic images and object surfaces for image guidance in neurosurgery *IEEE Trans. Med. Imaging* **21** 23–30

DiGioia A M, Jaramaz B and Colgan B D 1998 Computer assisted orthopaedic surgery: image guided and robotic assistive technologies *Clin. Orthop.* **354** 8–16

Downey D B, Fenster A and Williams J C 2000 Clinical utility of three-dimensional US *Radiographics* **20** 559–71

Drasic D and Milgram P 1996 Perceptual issues in augmented reality *Proc. SPIE 2653–19 Stereoscopic Displays and Virtual Reality Systems* 3rd edn (Bellingham, WA: SPIE (The International Society for Optical Engineering)) pp 123–34

Drebin R, Carpenter L and Hanrahan P 1988 Volume rendering *ACM Comput. Graph.* **22** 65–74

Edwards P J, Hawkes D J, Hill D L, Jewell D, Spink R, Strong A and Gleeson 1995 Augmentation of reality using an operating microscope for otolaryngology and neurosurgical guidance *J. Image Guid. Surg.* **1** 172–8

Edwards P J *et al* 1999 Stereo augmented reality in the surgical microscope *Stud. Health Technolo. Inform.* **62** 102–8

Edwards P J *et al* 2000 Design and evaluation of a system for microscope-assisted guided interventions (MAGI) *IEEE Trans. Med. Imaging* **19** 1082–93

Ehrhardt J, Handels H, Plotz W and Poppl S J 2004 Atlas-based recognition of anatomical structures and landmarks and the automatic computation of orthopedic parameters *Methods Inf. Med.* **43** 391–7

Englmeier K-H, Haubner M, Krapichler C, Seemann M and Reiser M 2000 Virtual reality and clinical applications *Progress in Medical Image Display and PACS* ed Y Kim and S Horri (Bellingham, WA: SPIE—The International Society for Optical Engineering) pp 67–102

Erhart P, Ladd M E, Steiner P, Heske N, Dumoulin C L and Debatin J F 1998 Tissue-independent MR tracking of invasive devices with an internal signal source *Magn. Reson. Med.* **39** 279–84

Fahrig R and Holdsworth D W 2000 Three-dimensional computed tomographic reconstruction using a C-arm mounted XRII: image-based correction of gantry motion nonidealities *Med. Phys.* **27** 30–8

Falk V, Jacobs S, Gummert J and Walther T 2003 Robotic coronary artery bypass grafting (CABG)–the Leipzig experience *Surg. Clin. North Am.* **83** 1381–6

Fenster A, Downey D B and Cardinal H N 2001 Three-dimensional ultrasound imaging *Phys. Med. Biol.* **46** R67–R99

Fenster A, Surry K J, Mills G R and Downey D B 2004 3D ultrasound guided breast biopsy system *Ultrasonics* **42** 769–74

Fichtinger G, Deguet A, Masamune K, Balogh E, Fischer G, Mathieu H, Taylor R, Fayad L M and Zinreich S J 2004 Needle insertion in CT scanner with image overlay—Cadaver studies *Proc. MICCAI 2004, LNCS 3217* ed C Barillot, D R Haynor and P Hellier (Berlin: Springer) pp 795–803

Figl M, Birkfellner W, Watzinger F, Wanschitz F, Hummel J, Hanel R, Ewers R and Bergmann H 2002 PC-based control unit for a head-mounted operating microscope for augmented reality visualization in surgical navigation *Proc. MICCAI 2002, LNCS 2489* ed T Dohi and R Kikinis (Berlin: Springer) pp 44–51

Figl M, Ede C, Hummel J, Wanschitz F, Ewers R, Bergmann H and Birkfellner W 2005 A fully automated calibration method for an optical see-through head-mounted operating microscope with variable zoom and focus *IEEE Trans. Med. Imaging* **24** 1492–9

Finnis K W, Starreveld Y P, Parrent A G, Sadikot A F and Peters T M 2003 A three-dimensional atlas of subcortical electrophysiology for the planning and guidance of functional neurosurgery *IEEE Trans. Med. Imaging* **21** 93–104

Fisher Y, Hanutsaha P, Tong S, Fenster A, Mazarin G and Mandava N 1998 Three-dimensional ophthalmic contact B-scan ultrasonography of the posterior segment *Retina* **18** 251–6

Fitzpatrick J M, West J B and Maurer C R J 1998 Predicting error in rigid-body point-based registration *IEEE Trans. Med. Imaging* **17** 694–702

Frangi A F, Rueckert D, Schnabel J A and Niessen W J 2002 Automatic construction of multiple-object three-dimensional statistical shape models: application to cardiac modeling *IEEE Trans. Med. Imaging* **21** 1151–66

Frantz D D, Wiles A D, Leis S E and Kirsch S R 2003 Accuracy assessment protocols for electromagnetic tracking systems *Phys. Med. Biol.* **48** 2241–51

Galloway R L Jr 2001 The process and development of image-guided procedures *Annu. Rev. Biomed. Eng.* **3** 83–108

George I, Mastrangelo M Jr, Hoskins J, Witzke W, Stich J, Garrison J, Witzke D B, Nichols M and Park A 2002 Using semi-automated image processing and desktop systems to incorporate actual patient volumetric data in immersive surgical planning and viewing systems for multiple patients *Stud. Health Technol. Inform.* **85** 155–9

Gering D T, Nabavi A, Kikinis R, Hata N, O'Donnell L J, Grimson W E, Jolesz F A, Black P M and Wells W M III 2001 An integrated visualization system for surgical planning and guidance using image fusion and an open MR *J. Magn. Resonan. Imaging* **13** 967–75

Gilani S, Norbash A M, Ringl H, Rubin G D, Napel S and Terris D J 1997 Virtual endoscopy of the paranasal sinuses using perspective volume rendered helical sinus computed tomography *Laryngoscope* **107** 25–9

Gilbert J C, Rubinsky B, Wong S T, Brennan K M, Pease G R and Leung P P 1997 Temperature determination in the frozen region during cryosurgery of rabbit liver using MR image analysis *Magn. Reson. Imaging* **15** 657–67

Giorgi C, Eisenberg H, Costi G, Gallo E, Garibotto G and Casolino D S 1995 Robot-assisted microscope for neurosurgery *J. Image Guid. Surg.* **1** 158–63

Gleason P L, Kikinis R, Altobelli D, Wells W, Alexander E, Black P M and Jolesz F 1994 Video registration virtual reality for nonlinkage stereotactic surgery *Stereotact. Funct. Neurosurg.* **63** 139–43

Gobbi D G and Peters T M 2002 Interactive interoperative 3D Ultrasound reconstruction and visualization *Medical Image Computing—Computer-Assisted Intervention MICCAI 2002, LNCS 2488* ed T Dohi and R Kikinis (Heidelberg: Springer) pp 156–63

Golfinos J and Spetzler R F 1996 The ISG system for 3-D craniotomy *A Textbook of Stereotactic and Functional Neurosurgery* ed P L Gildenberg and R N Tasker (Philadelphia: McGraw-Hill)

Guildenberg P L 1988 General concepts of stereotactic surgery *Modern Stereotactic Neurosurgery* ed L D Lunsford (Boston: Martinus Nijhoff) pp 3–12

Guiraudon G M 2005 *Universal cardiac introducer US Patent* 20,050,137,609

Hardy T and Koch J 1982 Computer-assisted stereotactic surgery *Appl. Neurophysiol.* **45** 396–8

Hardy T L, Koch J and Lassiter A 1983 Computer graphics with computerized tomography for functional neurosurgery *Appl. Neurophysiol.* **46** 217–26

Hemal A K and Menon M 2004 Robotics in urology *Curr. Opin. Urol.* **14** 89–93

Henri C J, Collins D L and Peters T M 1991a Multi-modality image integration for stereotactic surgery planning *Med. Phys.* **18** 167–77

Henri C J, Collins D L, Pike G B, Olivier A and Peters T M 1991b Clinical experience with a stereoscopic image workstation, *Proc. SPIE 1444 (San Jose, CA, USA)* (Bellingham, WA: International Society for Optical Engineering) pp 306–17

Herline A J, Herring J L, Stefansic J D, Chapman W C, Galloway R L Jr and Dawant B M 2000 Surface registration for use in interactive, image-guided liver surgery *Comput. Aided Surg.* **5** 11–7

Herline A J, Stefansic J D, Debelak J P, Hartmann S L, Pinson C W, Galloway R L and Chapman W C 1999 Image-guided surgery: preliminary feasibility studies of frameless stereotactic liver surgery *Arch. Surg.* **134** 644–9

Hernes T A, Ommedal S, Lie T, Lindseth F, Lango T and Unsgaard G 2003 Stereoscopic navigation-controlled display of preoperative MRI and intraoperative 3D ultrasound in planning and guidance of neurosurgery: new technology for minimally invasive image-guided surgery approaches *Minim. Invasive Neurosurg.* **46** 129–37

Hill D L, Batchelor P G, Holden M and Hawkes D J 2001 Medical image registration *Phys. Med. Biol.* **46** R1–R45

Hill D L G, Maurer C R, Maciunas R J, Barwise J A, Fitzpatrick J M and Wang M Y 1998 Measurement of intra-operative brain surface deformation under a craniotomy *Neurosurgery* **43** 514–28

Hill D L, Hawkes D J, Crossman J E, Gleeson M J, Cox T C, Bracey E E, Strong A J and Graves P 1991 Registration of MR and CT images for skull base surgery using point-like anatomical features *Br. J. Radiol.* **64** 1030–5

Hill D L, Hawkes D J, Gleeson M J, Cox T C, Strong A J, Wong W L, Ruff C F, Kitchen N D, Thomas D G and Sofat A 1994 Accurate frameless registration of MR and CT images of the head: applications in planning surgery and radiation therapy *Radiology* **191** 447–54

Hinks R S, Bronskill M J, Kucharczyk W, Bernstein M and Collick R M 1998 M R systems for image guided therapy *J. Magn. Reson. Imaging* **8** 19–25

Holm H H and Skjoldbye B 1996 Interventional ultrasound *Ultrasound Med. Biol.* **22** 773–899

Horsley V and Clarke R H 1908 The structure and function of the cerebellum examined by a new method *Brain* **31** 45–124

Hoult D I *et al* 2001 The engineering of an interventional MRI with a movable 1.5 Tesla magnet *J. Magn. Reson. Imaging* **13** 78–86

Hummel J B, Bax M R, Figl M L, Kang Y, Maurer C Jr, Birkfellner W W, Bergmann H and Shahdi R 2005 Design and application of an assessment protocol for electromagnetic tracking systems *Med. Phys.* **32** 2371–9

Hummel J, Figl M, Kollmann C, Bergmann H and Birkfellner W 2002 Evaluation of a miniature electromagnetic position tracker *Med. Phys.* **29** 2205–12

Johnson L G, Edwards P and Hawkes D 2003 Surface transparency makes stereo overlays unpredictable: the implications for augmented reality *Stud. Health Technol. Inform.* **94** 131–6

Kanner A A, Vogelbaum M A, Mayberg M R, Weisenberger J P and Barnett G H 2002 Intracranial navigation by using low-field intraoperative magnetic resonance imaging: preliminary experience *J. Neurosurg.* **97** 1115–24

Kant A J, Klein M D and Langenburg S E 2004 Robotics in pediatric surgery: perspectives for imaging *Pediatr. Radiol.* **34** 454–61

Kaspersen J H, Sjolie E, Wesche J, Asland J, Lundbom J, Odegard A, Lindseth F and Nagelhus Hernes T A 2003a Three-dimensional ultrasound-based navigation combined with preoperative CT during abdominal interventions: a feasibility study *Cardiovasc. Interv. Radiol.* **26** 347–56

Kaspersen J H, Sjolie E, Wesche J, Asland J, Lundbom J, Odegard A, Lindseth F and Nagelhus Hernes T A 2003b Three-dimensional ultrasound-based navigation combined with preoperative CT during abdominal interventions: a feasibility study *Cardiovasc. Interv. Radiol.* **26** 347–56

Kelly P J 1991 *Tumor Stereotaxis* (New York: Saunders)

Kelly P J 1986 Computer-assisted stereotaxis: new approaches for the management of intracranial intra-axial tumors *Neurology* **36** 535–41

Kelly J J, Hader W J, Myles S T and Sutherland G R 2005 Epilepsy surgery with intraoperative MRI at 1.5 T *Neurosurg. Clin. North Am.* **16** 173–83

Klotz H P, Flury R, Erhart P, Steiner P, Debatin J F, Uhlschmid G and Largiader F 1997a Magnetic resonance-guided laparoscopic interstitial laser therapy of the liver *Am. J. Surg.* **174** 448–51

Klotz H P, Flury R, Schonenberger A, Debatin J F, Uhlschmid G and Largiader F 1997b Experimental cryosurgery of the liver under magnetic resonance guidance *Comput. Aided Surg.* **2** 340–5

Koivukangas J, Louhisalmi Y, Alakuijala J and Oikarinen J 1993 Ultrasound-controlled neuronavigator-guided brain surgery *J. Neurosurg.* **79** 36–42

Kwoh Y S *et al* 1985 A new computerized tomographic-aided robotic stereotaxis system *Robot. Age* **7** 17–20

Kwoh Y S and Young R 1992 Robotic aided surgery *Computers in Stereotactic Neurosurgery* ed P J Kelly (Oxford, UK: Blackwell) pp 320–9

Lauriola W, Nardella M, Strizzi V, Cali A, D'Angelo V and Florio F 2005 3D angiography in the evaluation of intracranial aneurysms before and after treatment: initial experience *Radiol. Med.* **109** 98–107

Lemieux L, Jagoe R, Fish D R, Kitchen N D and Thomas D G 1994 A patient-to-computed-tomography image registration method based on digitally reconstructed radiographs *Med. Phys.* **21** 1749–60

Levoy M 1988 Direct visualization of surfaces from computed tomography data *Medical Imaging: Proc. SPIE 914* (Bellingham, WA: The International Society for Optical Engineering) pp 828–41

Levy R 1992 A short history of stereotactic neurosurgery Park Ridge, Ill, American Association of Neurological Surgeons. www.neurosurgery.org/Cybermuseum/stereotactichall/stereoarticle.html

Levy M L, Chen J C T, Moffart K, Corber Z and McComb J G 1998 Stereoscopic head-mounted display incorporated into microsurgical procedures *Neurosurgery* **43** 392–6

Liao H, Hata N, Iwahara M, Sakuma I and Dohi T 2003 An autostereoscopic display system for image-guided surgery using high-quality integral videography with high performance computing *Proc. MICCAI 2003, LNCS 2879* ed R E Ellis and T M Peters (Heidelberg: Springer) pp 247–55

Liao H, Hata N, Nakajima S, Iwahara M, Sakuma I and Dohi T 2004a Surgical navigation by autostereoscopic image overlay of integral videography *IEEE Trans. Inf. Technol. Biomed.* **8** 114–21

Liao H, Iwahara M, Hata N and Dohi T 2004b High-quality integral videography using a multiprojector *Opt. Express* **12** 1067–76

Lindseth F, Kaspersen J H, Ommedal S, Lango T, Bang J, Hokland J, Unsgaard G and Hernes T A 2003 Multimodal image fusion in ultrasound-based neuronavigation: improving overview and interpretation by integrating preoperative MRI with intraoperative 3D ultrasound *Comput. Aided Surg.* **8** 49–69

Livyatan H, Yaniv Z and Joskowicz L 2003 Gradient-based 2-D/3-D rigid registration of fluoroscopic X-ray to CT *IEEE Trans. Med. Imaging* **22** 1395–406

Lorensen W E and Cline H E 1987 Marching cubes: a high resolution 3D surface construction algorithm *ACM Comput. Graph.* **21** 163–9

Lorenzo-Valdes M, Sanchez-Ortiz G I, Elkington A G, Mohiaddin R H and Rueckert D 2004 Segmentation of 4D cardiac MR images using a probabilistic atlas and the EM algorithm *Med. Image Anal.* **8** 255–65

Louw D F, Fielding T, McBeth P B, Gregoris D, Newhook P and Sutherland G R 2004 Surgical robotics: a review and neurosurgical prototype development *Neurosurgery* **54** 525–367

Lunsford L D 1988 Magnetic resonance imaging stereotactic thalamotomy: report of a case with comparison to computed tomography *Neurosurgery* **23** 363–7

Machi J and Sigel B 1996 Operative ultrasound in general surgery *Am. J. Surg.* **172** 15–20

Maintz J B A and Viergever M A 1998 A survey of medical image registration *Med. Image Anal.* **2** 1–36

Masamune K, Fichtinger G, Patriciu A, Susil R C, Taylor R H, Kavoussi L R, Anderson J H, Sakuma I, Dohi T and Stoianovici D 2001 System for robotically assisted percutaneous procedures with computed tomography guidance *Comput. Aided Surg.* **6** 370–83

Mastrangelo M J Jr, Stich J, Hoskins J D, Witzke W, George I, Garrison J, Nichols M and Park A E 2002 Advancements in immersive VR as a tool for preoperative planning for laparoscopic surgery *Stud. Health Technol. Inform.* **85** 274–9

Maurer C R, Fitzpatrick J M, Wang M Y, Galloway R L, Maciunas R J and Allen G S 1997a Registration of head volume images using implantable fiducial markers *IEEE Trans. Med. Imaging* **16** 447–62

Maurer C R Jr *et al* 1998 Investigation of intraoperative brain deformation using a 1.5-T interventional MR system: preliminary results *IEEE Trans. Med. Imaging* **17** 817–25

Maurer C R J, Fitzpatrick J M, Wang M Y, Galloway R L J, Maciunas R J and Allen G S 1997b Registration of head volume images using implantable fiducial markers *IEEE Trans. Med. Imaging* **16** 447–62

Maurer C R J, Maciunas R J and Fitzpatrick J M 1998 Registration of head CT images to physical space using a weighted combination of points and surfaces *IEEE Trans. Med. Imaging* **17** 753–611

Mevis 2005 Mevis Hepatic Surgery Planning. Web Site 2005 http://www.mevis.de/projects/liver/page_5.html

Miga M, Paulsen K, Kennedy F, Hoopes J, Hartov A and Roberts D W 2000 Initial in-vivo analysis of 3-D heterogeneous brain computations for model-updated image-guided neurosurgery *Proc. MICCAI 2000, LNCS 1496* ed W M Wells, A Colchester and S Delp (Berlin: Springer) pp 743–52

Miga M I, Sinha T K, Cash D M, Galloway R L and Weil R J 2003 Cortical surface registration for image-guided neurosurgery using laser-range scanning *IEEE Trans. Med. Imaging* **22** 973–85

Morita A and Kelly P J 1993 Resection of intraventricular tumors via a computer-assisted volumetric stereotactic approach *Neurosurgery* **32** 920–6

Moriarty T M, Kikinis R, Jolesz F A, Black P M and Alexander E 1996 Magnetic resonance imaging therapy: intraoperative MR imaging *Neurosurg. Clin. North Am. Apr.* **7** 323–31

Moulder C, Sati M, Wentkowski M V and Nolte L P 2003 A transcutaneous bone digitizer for minimally invasive registration in orthopedics: a real-time focused ultrasound beam approach *Comput. Aided Surg.* **8** 120–8

Munz Y, Moorthy K, Dosis A, Hernandez J D, Bann S, Bello F, Martin S, Darzi A and Rockall T 2004 The benefits of stereoscopic vision in robotic-assisted performance on bench models *Surg. Endosc.* **18** 611–6

Novick R J, Fox S A, Kiaii B B, Stitt L W, Rayman R, Kodera K, Menkis A H and Boyd W D 2003 Analysis of the learning curve in telerobotic, beating heart coronary artery bypass grafting: a 90 patient experience *Annal. Thorac. Surg.* **76** 749–53

Nowinski W L, Fang A, Nguyen B T, Raphel J K, Jagannathan L, Raghavan R, Bryan R N and Miller G A 1998 Multiple brain atlas database and atlas-based neuroimaging system *Comput. Aided Surg.* **2** 42–66

Nowinski W L, Yeo T T and Yang G L 1997 Atlas-based system for functional neurosurgery *Proc. SPIE Medical Imaging 1997: Image Display* ed Y Kim (Bellingham WA: SPIE—The International Society for Optical Engineering) pp 92–103

Olivier A, Alonso-Vanegas M, Comeau R and Peters T M 1996 Image-guided surgery of epilepsy *Neurosurg. Clin. North Am.* **7** 229–43

Olivier A, Bertrand G and Picard C 1983 Discovery of the first human stereotaxic instrument *Appl. Neurophysiol.* **46** 84–91

Olivier A, Germano I M, Cukiert A and Peters T 1994 Frameless stereotaxy for surgery of the epilepsies: preliminary experience *J. Neurosurg.* **81** 629–33

Park H, Bland P H and Meyer C R 2003 Construction of an abdominal probabilistic atlas and its application in segmentation *IEEE Trans. Med. Imaging* **22** 483–92

Paul H A, Bargar W L, Mittlestadt B, Musits B, Taylor R H, Kazanzides P, Zuhars J, Williamson B and Hanson W 1992 Development of a surgical robot for cementless total hip arthroplasty *Clin. Orthop. Rel. Res.* **285** 57–66

Pelizzari C A, Chen G T Y, Spelbring D R, Weichselbaum R R and Chen C T 1989 Accurate three-dimensional registration of PET, CT and MR images of the brain *J. Comput. Assist. Tomogr.* **13** 20–6

Peters T M, Clark J A, Olivier A, Marchand E P, Mawko G, Dieumegarde M, Muresan L V and Ethier R 1986 Integrated stereotaxic imaging with CT, MR imaging and digital subtraction angiography *Radiology* **161** 821–6

Peters T M, Davey B L K, Munger P, Comeau R, Evans A C and Olivier A 1996 Three-dimensional multimodal image-guidance for neurosurgery *IEEE Trans. Med. Imaging* **15** 121–8

Peters T M, Henri C J, Munger P, Takahashi A M, Evans A C, Davey B and Oliver A 1994 Integration of stereoscopic DSA and 3D MRI for image-guided neurosurgery *Comput. Med. Imaging Graph.* **18** 289–99

Qatarneh S M, Noz M E, Hyodynmaa S, Maguire G Q Jr, Kramer E L and Crafoord J 2003 Evaluation of a segmentation procedure to delineate organs for use in construction of a radiation therapy planning atlas *Int. J. Med. Inform.* **69** 39–55

Radetzky A, Schrocker F and Auer L M 2000 Improvement of surgical simulation using dynamic volume rendering *Stud. Health Technol. Inform.* **70** 272–8

Reinhardt H F, Horstmann G A, Trippel M and Westermann B 1998 Sonic triangulation systems *Textbook of Stereotactic and Functional Neurosurgery* ed P L Guildenberg and R N Tasker (New York: McGraw-Hill) pp 221–4

Rickers C *et al* 2004 Applications of magnetic resonance imaging for cardiac stem cell therapy *J. Intervent. Cardiol.* **17** 37–46

Rickers C, Jerosch-Herold M, Hu X, Murthy N, Wang X, Kong H, Seethamraju R T, Weil J and Wilke N M 2003 Magnetic resonance image-guided transcatheter closure of atrial septal defects *Circulation* **107** 132–8

Robb R A 1999 3-D visualization in biomedical applications *Annu. Rev. Biomed. Eng.* **1** 377–99

Robb R A 2002 Three-dimensional visualization and analysis in prostate cancer *Drugs Today* **38** 153–65

Robb R A, Hanson D P, Karwoski R A, Larson A G, Workman E L and Stacy M C 1989 Analyze: a comprehensive, operator-interactive software package for multidimensional medical image display and analysis *Comput. Med. Imaging Graph.* **13** 433–54

Roberts D W and Darcey T M 1996 The evaluation and image-guided surgical treatment of the patient with a medically intractable seizure disorder *Neurosurg. Clin. North Am.* **7** 215–27

Roberts D W, Hartov A, Kennedy F E, Miga M I and Paulsen K D 1998 Intraoperative brain shift and deformation: a quantitative analysis of cortical displacement in 28 cases *Neurosurgery* **43** 749–58

Rohling R N, Gee A H and Berman L 1998 Automatic registration of 3-D ultrasound images *Ultrasound Med. Biol.* **24** 841–54

Russakoff D B, Rohlfing T, Mori K, Rueckert D, Ho A, Adler J R Jr and Maurer C R Jr 2005 Fast generation of digitally reconstructed radiographs using attenuation fields with application to 2D–3D image registration *IEEE Trans. Med. Imaging* **24** 1441–54

Saiviroonporn P, Robatino A, Zahajszky J, Kikinis R and Jolesz F A 1998 Real-time interactive three-dimensional segmentation *Acad. Radiol.* **5** 49–56

Sakurai H *et al* 2004 CT-fluoroscopy guided interstitial brachytherapy with image-based treatment planning for unresectable locally recurrent rectal carcinoma *Brachytherapy* **3** 222–30

Sawaya R, Rambo W M Jr, Hammoud M A and Ligon B L 1995 Advances in surgery for brain tumors *Neurol. Clin.* **13** 757–71

Schaltenbrand G and Wahren P 1977a *Introduction to Stereotaxis with an Atlas of the Human Brain* (Stuttgart: Thieme)

Schaltenbrand G and Wahren W 1977b *Atlas for Stereotaxy of the Human Brain* (Stuttgart: Thieme)

Schenck J F, Jolesz F A, Roemer P B, Cline H E, Lorensen W E, Kikinis R, Silverman S G, Hardy C J, Barber W D and Laskaris E T 1995 Superconducting open-configuration MR imaging system for image-guided therapy *Radiology* **195** 805–14

Schoenhagen P, Stillman A E, Halliburton S S, Kuzmiak S A, Painter T and White R D 2005 Non-invasive coronary angiography with multi-detector computed tomography: comparison to conventional X-ray angiography *Int. J. Cardiovasc. Imaging* **21** 63–72

Schroeder W J, Avila L S and Hoffman W 2000 Visualizing with VTK: a tutorial *IEEE Comput. Graph. Appl.* **20** 20–7

Schulder M, Sernas T J and Carmel P W 2003 Cranial surgery and navigation with a compact intraoperative MRI system *Acta Neurochirurg.* Suppl. **85** 79–86

Shahidi R, Bax M R, Maurer C R Jr, Johnson J A, Wilkinson E P, Wang B, West J B, Citardi M J, Manwaring K H and Khadem R 2002 Implementation, calibration and accuracy testing of an image-enhanced endoscopy system *IEEE Trans. Med. Imaging* **21** 1524–35

Shahidi R, Mezrich R and Silver D 1995 Proposed simulation of volumetric image navigation using a surgical microscope *J. Image Guid. Surg.* **1** 249–65

Shimizu K, Mulkern R V, Oshio K, Panych L P, Yoo S S, Kikinis R and Jolesz F A 1998 Rapid tip tracking with MRI by a limited projection reconstruction technique *J. Magn. Reson. Imaging* **8** 262–4

Siewerdsen J H, Moseley D J, Burch S, Bisland S K, Bogaards A, Wilson B C and Jaffray D A 2005 Volume CT with a flat-panel detector on a mobile, isocentric C-arm: pre-clinical investigation in guidance of minimally invasive surgery *Med. Phys.* **32** 241–54

Smolikova-Wachowiak R, Wachowiak M P, Fenster A and Drangova M 2005 Registration of two-dimensional cardiac images to preprocedural three-dimensional images for interventional applications *J. Magn. Reson. Imaging* **22** 219–28

Soler L, Delingette H, Malandain G, Montagnat J, Ayache N, Koehl C, Dourthe O, Malassagne B, Smith M, Mutter D and Marescaux J 2001 Fully automatic anatomical, pathological, and functional segmentation from CT scans for hepatic surgery *Comput. Aided Surg.* **6** 131–42

Solomon S B, Patriciu A, Bohlman M E, Kavoussi L R and Stoianovici D 2002 Robotically driven interventions: a method of using CT fluoroscopy without radiation exposure to the physician *Radiology* **225** 277–82

Spiegel E A, Wycis H T, Marks M and Lee A S 1947 Stereotaxic apparatus for operation of the human brain *Science* **106** 349–50

St-Jean P, Sadikot A F, Collins D L, Clonda D, Kasrai R, Evans A C and Peters T M 1998 Automated atlas integration and interactive 3-dimensional visualization tools for planning and guidance in functional neurosurgery *IEEE Trans. Med. Imaging* **17** 672–80

Stefansic J D, Herline A J, Chapman W C and Galloway R L Jr 1998 Endoscopic tracking for use in interactive image-guided surgery *Proc. SPIE: Medical Imaging 3335* (Bellingham, WA: Society of Photo-optical and Instrumentation Engineers) pp 208–18

Steiner P, Erhart P, Heske N, Dumoulin C L, von Schulthess G K and Debatin J F 1997 Active biplanar MR tracking for biopsies in humans *Am. J. Roentgenol.* **169** 735–8

Steinmeier R, Fahlbusch R, Ganslandt O, Nimsky C, Buchfelder M, Kaus M, Heigl T, Lenz G, Kuth R and Huk W 1998 Intraoperative magnetic resonance imaging with the magnetom open scanner: concepts, neurosurgical indications, and procedures: a preliminary report *Neurosurgery* **43** 739–48

Stetten G, Cois A, Chang W, Shelton D, Tamburo R, Castellucci J and Von Ramm O 2003 C-mode real time tomographic reflection for a matrix array ultrasound sonic flashlight *Proc. MICAI 2003, LNCS 2879* (Heidelberg: Springer) pp 336–43

Strother C M 2000 Interventional neuroradiology *Am. J. Neuroradiol.* **21** 19–24

Sugano N 2003 Computer-assisted orthopedic surgery *J. Orthop. Sci.* **8** 442–8

Sutherland G R, Kaibara T and Louw D F 2003 Intraoperative MR at 1.5 Tesla–experience and future directions *Acta Neurochirurg.* Suppl. **85** 21–8

Szpala S, Wierzbicki M, Guiraudon G and Peters T 2005 Real-time fusion of endoscopic views with dynamic 3D cardiac images: a phantom study *IEEE Trans. Med. Imaging* **24** 1207–15

Talairach J and Tourneau P 1988 *Co-planar stereotaxic atlas of the human brain* (Stuttgart: Georg Thieme Verlag)

Talairach J and Tourneau P 1993 *Referentially oriented cerebral MRI anatomy* (Georg Thieme Stuttgart: Verlag)

Tang T S Y and Ellis R E 2005 2D/3D registration using a hybrid atlas *Proc. MICCAI 2005, LNCS 3750* ed J Duncan and G Gerig (Heidelberg: Springer) pp 902–9

Thompson C J and Bertrand G 1972 A computer program to aid the neurosurgeon to locate probes used during stereotaxic surgery on deep cerebral structures *Comput. Programs Biomed.* **2** 265–76

Tokuda J, Morikawa S, Dohi T and Hata N 2004 Motion tracking in MR-guided liver therapy by using navigator echoes and projection profile matching *Acad. Radiol.* **11** 111–20

Tomazevic D, Likar B, Slivnik T and Pernus F 2003 3-D/2-D registration of CT and MR to X-ray images *IEEE Trans. Med. Imaging* **22** 1407–16

Tonet O, Megali G, Dario P, Carrozza M C, Marcacci M and La Palombara P F 2000 A novel navigation system for computer assisted orthopaedic surgery *Proc. 22nd Int. Conf. Medical and Biological Engineering Soc (IEEE, Chicago)* pp 1864–5

Trobaugh J W, Trobaugh D J and Richard W D 1994 Three-dimensional imaging with stereotactic ultrasonography *Comput. Med. Imaging Graph.* **18** 315–23

Tronnier V M, Wirtz C R, Knauth M, Bonsanto M M, Hassfeld S, Albert F K and Kunze S 1996 Intraoperative computer-assisted neuronavigation in functional neurosurgery *Stereotact. Funct. Neurosurg.* **66** 65–8

Turgeon G A, Lehmann G, Guiraudon G, Drangova M, Holdsworth D and Peters T M 2005 2D–3D registration of coronary angiograms for cardiac procedure planning and guidance *Med. Phys.* **32** 3737–49

van Vaals J J 1998 Interventional MR with a hybrid high-field system *Interventional Magnetic Resonance Imaging* ed J F Debatin and G Adam (Berlin: Springer) pp 19–32

Vetter M, Hassenpflug P, Thorn M, Cardenas C, Richter G M, Lamade W, Herfarth C and Meinzer H P 2002 Evaluation of visualization techniques for image-guided navigation in liver surgery *Stud. Health Technol. Inform.* **85** 536–41

Vining D J 1996 Virtual endoscopy: is it reality? *Radiology* **200** 30–1

Vogt S, Khamene A, Niemann H and Sauer F 2004 An AR system with intuitive user interface for manipulation and visualization of 3D medical data *Stud. Health Technol. Inform.* **98** 397–403

Wachowiak M P and Peters T M 2006 High performance medical image registration using optimization techniques *IEEE Trans. Inform. Technol. Biomed.* **10** 344–53

Webb S 1988 *The Physics of Medical Imaging* (Bristol: Adam Hilder)

Wei Z, Wan G, Gardi L, Mills G, Downey D and Fenster A 2004 Robot-assisted 3D-TRUS guided prostate brachytherapy: system integration and validation *Med. Phys.* **31** 539–48

Wiles A D, Thompson D G and Frantz D D 2004 Accuracy assessment and interpretation for optical tracking systems *Proc. SPIE* **5367** 421–32

Wilheim D, Feussner H, Schneider A and Harms J 2003 Electromagnetically navigated laparoscopic ultrasound *Surg. Technol. Int.* **11** 50–4

Wood B J *et al* 2005 Navigation with electromagnetic tracking for interventional radiology procedures: a feasibility study *J. Vasc. Interven. Radiol.* **16** 493–505

Worthington C, Peters T M, Ethier R, Melanson D, Theron J, Villemure J-G, Olivier A, Clark J and Mawko G 1985 Stereoscopic digital subtraction angiography in neurologic assessment *Am. J. Neuroradiol.* **6** 802–8

Yoo T S and Ackerman M J 2005 Open source software for medical image processing and visualization *Commun. ACM* **48** 55–9

Zhang Q, Chung Y C, Lewin J S and Duerk J L 1998 A method for simultaneous RF ablation and MRI *J. Magn. Reson. Imaging* **8** 110–4

Zinreich S J, Tebo S A, Long D M, Brem H, Mattox D E, Loury M E, vander Kolk C A, Koch W M, Kennedy D W and Bryan R N 1993 Frameless stereotaxic integration of CT imaging data: accuracy and initial applications *Radiology* **188** 735–42